



Research Papers

Conceptual review and optimization of liquid air energy storage system configurations for large scale energy storage

Gianluca Carraro^{a,*}, Piero Danieli^b, Tazio Boatto^a, Andrea Lazzaretto^a

^a Dept. of Industrial Engineering, University of Padova, Via Venezia 1, 35131 Padova, Italy

^b Dept. of Management and Engineering, University of Padova, Stradella S. Nicola 3, 36100 Vicenza, Italy



ARTICLE INFO

Keywords:

Liquid air energy storage
System configurations
HEATSEP method
Design optimization
Conceptual development

ABSTRACT

Among energy storage systems, Liquid Air Energy Storage (LAES) is attractive because of high energy density, ease of being scaled up, absence of geographical constraints, mature technology and use of safe materials/working fluids. This work presents a critical review of LAES system configurations in the literature to identify the criteria behind their conceptual development. The goal is achieved following the HEATSEP methodology, which allowed identifying a common thread in the evolution of all LAES configurations in the literature based on very few layouts, named “basic configurations”. The optimization of these few layouts, taking into account all possible internal heat transfers, provides a unique and comprehensive overview of existing configurations in spite of their seemingly great complexity. This picture clearly indicates the link between topology and performance improvement and provides insight into the limits of the maximum possible performance gain over the existing literature. The optimal results show that the margin for improvement is quite narrow. In the case of a complete thermal integration between charge and discharge phases with the addition of Organic Rankine Cycle system a gain from 61.9 % to 64.3 % is obtained over the best performing configuration in the literature.

1. Introduction

In electricity storage, electricity is converted into a form that can be stored and later converted back into electricity when needed [1]. This process allows electricity to be generated during periods of low demand, low cost of generation or from intermittent energy sources, and used during periods of high demand, high cost of generation or when no other means of generation is available.

At the beginning of the 20th century, the traditional mode of operation of electric grids was aimed at matching a highly agglomerated demand with a small number of power generation systems, mainly hydroelectric power stations plus a few thermal power plants [2]. In this arrangement, peaks in the demand were smoothed by the large numbers of users, the energy demand of which was predictable by using long term statistics and so, a stable and secure service was guaranteed.

Nowadays, in many developed countries, a constantly increasing share of electrical energy is generated by renewable energy sources (RES), which pose many management and control issues [3] because of the intrinsic random nature of most of them. Electrical grids with large penetration of RES are now facing new problems: the deployment of power generation systems has not been imposed by large utilities, but by

residential and small industrial users, with significant unbalances between supply and demand capacity [4]. The new systems suffer from a double mismatch between supply and demand that are hard to predict because of i) smaller and local aggregation of the demand [5] and ii) the increasing penetration of intermittent RES in the supply systems [6]. The problems described above are likely to intensify due to the expected increase of energy systems based on RES, according to the present trends of European Union legislations on greenhouse gases emissions.

In this context, energy storage systems can play a fundamental role in decoupling energy demand and supply [7]. Among energy storage systems for large scale applications only a few do not depend on geographical and environmental conditions and so, are effectively utilizable everywhere [8–10]. Liquid Air Energy Storage (LAES) systems have attracted significant attention in recent years not only for the absence of geographical constraints, but also for high energy densities, mature technology and use of safe materials/working fluids [11]. In LAES systems, the air liquefaction process is used to convert the energy into liquid air that is stored in cryogenic tanks and then, when needed, is regasified and expanded in turbines to generate electricity. LAES systems can be seen as an evolution of compressed air energy storage (CAES) systems where the compression and expansion work are shifted in time by storing air. The main advantage of LAES over CAES is that the

* Corresponding author.

E-mail address: gianluca.carraro@unipd.it (G. Carraro).

Nomenclature**Symbols and abbreviations**

LAES	Liquid Air Energy Storage
p	pressure, bar
T	temperature, K
\dot{m}	mass flow rate, kg/s
$\dot{Q}, \Delta H$	thermal power, kW
h	specific enthalpy, kJ/kg
P	power, kW
w	specific work, kJ/kg
E	energy, kWh
TIT	turbine inlet temperature, K
y	liquid yield, –
HCC	Hot Composite Curve
CCC	Cold Composite Curve

ORC	Organic Rankine Cycle
HEN	Heat Exchanger Network

Greek symbols

η	efficiency
Δ	difference

Subscripts

rt	round trip
is	isentropic
ch	charge cycle
dis	discharge cycle
c	compressor
e	cryogenic expander
pp	pump
t	turbine
in	inlet
out	outlet

working fluid is stored in liquid form, which greatly reduces its specific volume, and hence the storage tank volume. The use of air as storage medium is advantageous because the atmosphere itself represents the gaseous reservoir. In general, the LAES systems configurations can be divided into two main categories: i) systems relying on an external heat source (apart from the environment) that can be obtained by a power plant, waste heat from industrial processes or combustion with the working air; ii) self-sufficient systems.

The use of liquid air as an energy storage can be dated back to 1977, when it was first proposed by the University of Newcastle upon Tyne [12]. The first industrial interest on this technology came from Mitsubishi Heavy Industries and Hitachi during the 1990s. The pioneering work of Kishimoto et al. [13] proposed a system in which liquid air is stored in a tank and subsequently expanded when electricity is needed. In that system there was no integration between charging and discharging phase because the liquid air production relied on an already existing liquefaction plant that is not part of the study. The discharge phase is an open-loop Rankine cycle, in which heat is provided by the combustion of a fuel and utilizing the discharged air as oxidant. In the same period, Chino et al. [14] proposed a similar system, which, however, included both the air liquefaction and power recovery sections, so suggesting an integration between charge and discharge phases. The liquefaction cycle is a Claude cycle, in which a fraction of the compressed air is cooled down, expanded in a cryo-turbine and mixed with the vapour coming from the tank that is recirculated back to cool down the compressed. Both References [13, 14] declared efficiencies over 70 %.

Starting from 2005, the LAES technology has received substantial progresses from a collaborative research between the University of Leeds and Highview Enterprises Ltd. This research led to the design and construction of the world's first LAES pilot plant (350 kW/2.5 MWh) between 2009 and 2012. Morgan et al. [15] described the layout and operation of such plant: the liquefaction section consists of a modified Claude cycle with a recirculating compressor; the power recovery section is an air Rankine cycle that receives low temperature (70 °C) waste heat from industrial processes. The thermal integration of charge and discharge phases occurs via a cold thermal storage in which the evaporation of liquid air during the discharge process is used to store cold, which subsequently helps precool the air during the charge process (this is also referred as “cold recycling”). The plant achieved a roundtrip efficiency of just 8 % because of the small size, the non-optimal operation parameters and the partial internal cold exergy recovery. Nonetheless, this demonstrative plant showed the feasibility of developing a new storage system using commercially available technologies.

Li et al. [16] in 2013 proposed further developments of the LAES system concept in [15], which include the following differences: a)

downstream of the expanders, air is heated by the cooling systems of a pressurized water nuclear reactor instead of low temperature waste heat recovery; b) air liquefaction is obtained with a Solvay cycle. The thermal integration between charge and discharge phases comprises the cold recycling, and the declared efficiency is about 71 %. This efficiency is not defined in the conventional way, i.e., as ratio between the power produced in the discharge phase and that consumed in the charge phase, but as ratio between the increased power output supplied by LAES (compared to the normal power production of the nuclear reactor) and the power consumed for the liquid air production.

In 2015, Guizzi et al. [17] proposed a plant layout that does not rely on waste heat or other external heat sources, uses a Solvay liquefaction cycle, and achieves a roundtrip efficiency of 55 %. The novelty of this work was the increased thermal integration via hot recycling in addition to cold recycling. Hot air exiting the compressor allows storing heat in a hot thermal storage during charging and then the thermal storage heats up the air entering the turbines during discharge. A similar plant layout has been proposed in the work of Guo et al. [18] (in which the authors declare 67 % of roundtrip efficiency), Sciacovelli et al. [19] (48 %) and Hamdy et al. [20] (40 %).

Other works proposed the integration of an ORC system into LAES using several methods. She et al. [21] proposed a layout similar to that in [17], and placed a R32 ORC system using the LAES hot storage (charged from hot compressed air) as thermal source and rejecting heat to the evaporator of a vapour compression cycle. The authors showed an increase in roundtrip efficiency from 50 % to 55 % with the addition of the ORC system. In 2018, Tafone et al. [22] proposed two different layouts of ORC integration with the LAES system: the first called “LAORC1”, in which the R134a evaporator receives heat from the hot storage in series (downstream) with air superheater; the second called “LAORC2”, in which the R245fa evaporator is in parallel with air superheater. The authors claimed a roundtrip efficiency of 48 % for the baseline configuration, 50.5 % for LAORC1 and 52.9 % LAORC2 ones. Hamdy et al. [20] compared the performance of different configurations including ORC systems in different ways. They found that without exploiting the cold recycling, the ORC was detrimental to the roundtrip efficiency.

Most of the current research efforts on LAES system configurations focus on performance evaluation of specific configurations (as seen above), parametric analyses [23], integration into multi energy systems [24,25], first economic analyses [26,27] and coupling of the most advanced configurations with other energy systems such as thermo-electric generators [28], LNG gasification system, combined cycles [29], desalination systems [30]. Adejebi et al. [31] proposed the addition of a desiccant wheel dehumidifier and a cooling heat exchanger to treat the air entering the compression train of the LAES system. They found out that the reduction of both relative humidity (from about 80 % to 10 %)

and temperature (from ambient to 10 °C) of the inlet air improves the round-trip efficiency of up to 11.7 % due to a strong decrease of the compression work. Wang et al. [32] evaluated a simplified LAES “cold box”, which uses only one pressurized fluid (propane at 10 bar) instead of using two different fluids (as typically done) to maximize the cold energy recovery in a wide temperature range (from 85 K of liquid air to 300 K of ambient temperature). This solution increases the cold storage density, simplifies the overall structure of the system and, in turn, reduces the investment costs. Yang et al. [33] studied the performance improvement of a LAES system coupled with a solar tower, which supplies heat to the thermal oil of the high temperature storage linking heat rejection from the charge process and heat addition to the discharge process. The temperature gain given by the heat addition improved the round-trip efficiency up to 30 %. Nabat et al. [34] integrated a LAES system with several energy conversion units to enhance the penetration of renewable energy. In particular, a Kalina cycle system and thermoelectric generators exploit the excess heat coming from the compression train, while high temperature energy storages (HTES) supply high grade heat (up to 1250 K) to air in the discharge process. This system allows handling renewable power generation in a more flexible way since extra power coming from renewables can charge both the LAES system and HTES. The total system achieved a round-trip efficiency of 61.6 %.

A broader view on LAES system configurations is given either in review papers or in works that optimize and compare different configurations under the same boundary conditions. Although complete in presenting the state-of-the-art of LAES systems in all aspects, review papers usually address configurations by decomposing LAES in its basic elements to show and explain each of them, i.e., charge phase (or liquefaction cycle), storage section, thermal energy recovery and discharge phase [35], and then grouping the configurations available in the literature according to role and application of LAES, i.e., standalone or integrated with surrounding energy systems [36]. On the other hand, papers evaluating different LAES configurations consider specific features as terms of comparison, such as the integration of ORC systems [20,22].

It is clear that, on one hand, review papers lack an in-depth thermodynamic analysis that puts the accent on the principles guiding the conceptual development of all LAES system configurations. On the other hand, papers dealing with thermodynamic comparisons of different configurations lack a complete overview of the evolution of configurations that helps identify the reasons and advantages of optimizing their specific features.

This work combines the approach of a review on LAES system configurations with that of an in-depth thermodynamic analysis to fill in the above-mentioned gaps. In particular, it carries out a critical review of all the configurations proposed in the literature, using a new methodology to identify general criteria behind the evolution of LAES systems. This methodology: *i*) assumes that the charging and discharging of the system occur simultaneously (with the thermal storage acting as a temporal link between the two sections), *ii*) utilizes Pinch Analysis techniques [37] to simplify the evaluation of internal thermal integration, *iii*) exploits the HEATSEP method [38,39] to obtain the best match between hot and cold flows available internally, therefore improving the round-trip efficiency of the considered systems.

The goals of this work are:

1. Analyse the system layouts proposed in the literature to identify a common thread in their evolution.
2. Carry out an in-depth investigation of the internal heat transfer to understand potential and limits of the configurations available in the literature.
3. Evaluate possible further performance improvements of these layouts.
4. Supply a complete and “easy to read” overview of all existing configurations using a common “language”.

These goals are achieved as shown in the flowchart in Fig. 1. The work starts with a review of the numerous, and increasingly complex, LAES configurations, which is carried out in Section 3. This starting point is necessary to understand the evolution of LAES configurations and “extract” their basic structures, understood as an assembly of compression and expansion stages and their interconnections (referred to as “basic configurations”). This part shows that despite the large number of configurations presented in the literature, their basic configurations are very few. Identifying these representative core configurations is the basis for the subsequent application of the HEATSEP method to find the best internal heat transfer, thus showing whether there may be room for improvement over the literature results (we remind that HEATSEP stands for separation “SEP” of the heat transfer “HEAT” problem in the synthesis of a thermal system configuration [38]). The achievement of the optimal internal heat transfer is checked using the thermal composite curves at system level, a very useful tool not commonly used in the existing literature of LAES systems although extensively utilized in the analysis and optimization of many other complex systems configurations, since the development of Pinch Analysis [37].

The order in which the final optimal configurations are obtained is the following:

- Section 4 shows the evolution of the LAES configurations in the literature, which is addressed according to a step by step increase of complexity. At each step, the reasons for the layout modifications are deeply investigated.
- Section 5 describes the details of LAES system modeling, mathematical formulation of the optimization problems and explanation of the HEATSEP method applied to LAES systems.
- Section 6 shows the process to extract the “basic configurations”, related to all components different from the internal heat exchangers, from each group of configurations under the same evolution step [40]. The aim is that of grouping all configurations available in the literature into few representative basic layouts to be optimized [41,42].
- Section 7 presents an in-depth analysis and discussion on how optimal thermal composite curves (calculated by the HEATSEP optimization) of LAES internal heat transfers modify as the number of compression and expansion stages and the level of thermal integration change.
- Section 7 compares under the same boundary conditions the performance of all configurations of standalone LAES available in the literature with the performance evaluated by the optimization of the “basic configurations” according to the HEATSEP method.

2. The LAES system and performance metrics

LAES is an energy storage system based on liquid air. It works according to three main phases:

- i. Charge phase: liquid air is produced by means of a liquefaction cycle.
- ii. Storage phase: liquid air is stored in a cryogenic tank.
- iii. Discharge phase: liquid air is used as working fluid into a power generation cycle.

Fig. 2 shows the simplest layout of the LAES system, in which the charge phase includes a compressor, a heat exchanger and a throttling valve, the storage phase a cryogenic tank and the discharge phase a pump, a heat exchanger and a turbine. Table 1 shows the thermodynamic properties of air both at critical point and at the saturation pressure equal to the ambient one.

In the charge cycle, ambient air is first compressed (1–2, Figs. 2 and 3 (a)) in a compressor (usually a multistage compressor train) and then cooled down (2–3) before the expansion process (3–4) in a throttling

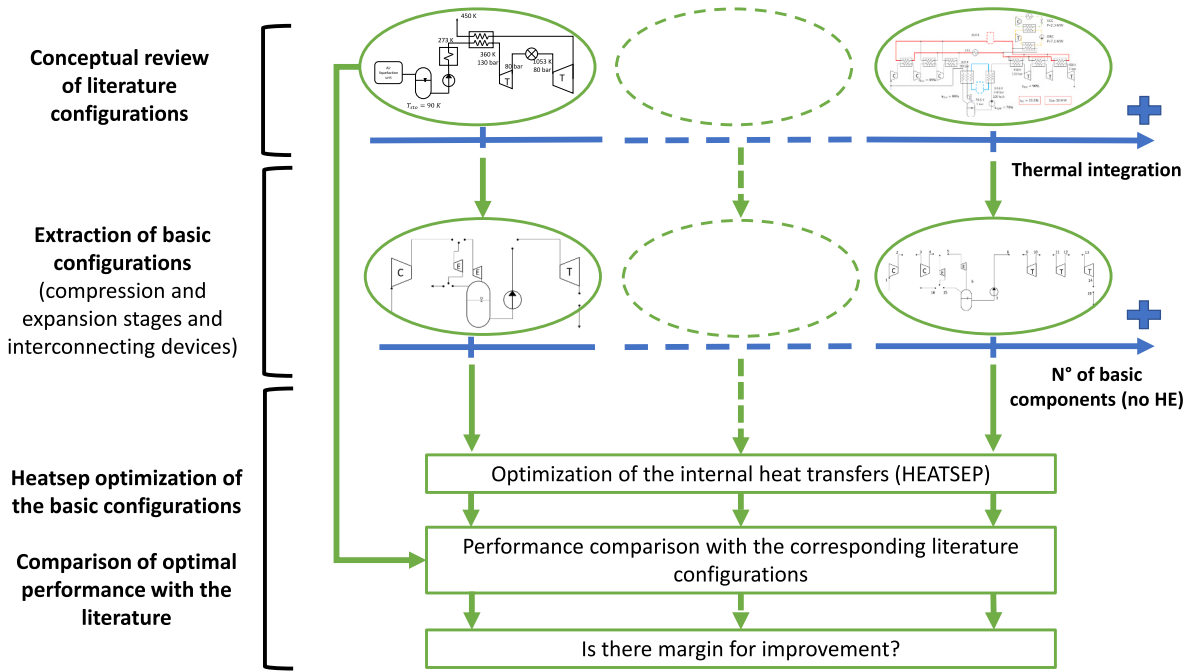


Fig. 1. Layout of the work structure.

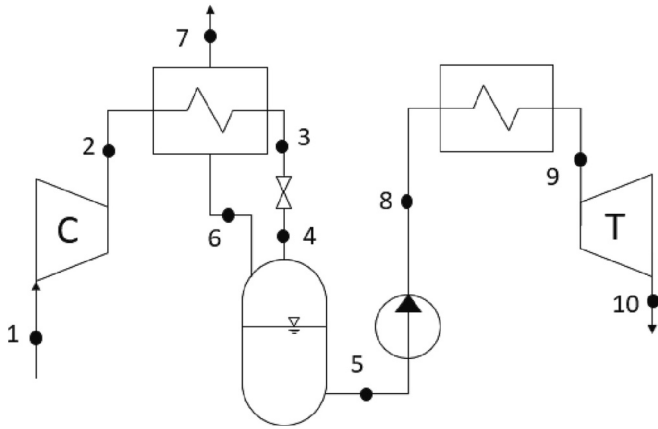


Fig. 2. The simplest LAES system layout.

Table 1

Critical point and properties of air at the saturation pressure equal to the ambient one.

Parameter [Unit]	Value
$T_{critical}$ [K]	132.83
$P_{critical}$ [bar]	38.50
T_{dew} [K]	81.75
T_{bubble} [K]	78.93
ρ_{liquid} [kg/m ³]	877.25
ρ_{vapour} [kg/m ³]	4.49

valve or a cryo-expander. After the expansion, a two-phase mixture is obtained (point 4). The liquid fraction is stored in a cryogenic tank (storage phase), whereas the gas phase fraction is used to cool down the compressed air (6–7) before the expansion.

In the discharge phase, the liquid air is pumped and subsequently heated to the gaseous phase, and finally expanded by the turbines generating power.

The main performance parameter for an energy storage system is the

round trip efficiency, which is generally defined as the ratio between energy released by the system in the discharge phase and the energy used to charge the system (based on a full charge and full discharge):

$$\eta_{rt} = \frac{E_{dis}}{E_{ch}} \quad (1)$$

Assuming that the charge time of the system is equal to discharge time, the round trip efficiency can be written in terms of power as:

$$\eta_{rt} = \frac{P_{dis}}{P_{ch}} \quad (2)$$

For the LAES system in Fig. 2, η_{rt} is defined as in Eq. (3), in which the discharge power is the difference between the turbine power output (P_t) and the pump power consumption (P_{pp}), whereas the charge power is the power consumed by the compressor (P_c):

$$\eta_{rt} = \frac{P_t - P_{pp}}{P_c} \quad (3)$$

In case the throttling valve between points 3–4 in Fig. 2 is replaced with a cryogenic expander (in the following called “cryo-expander”), Eq. (3) becomes:

$$\eta_{rt} = \frac{P_t - P_{pp}}{P_c - P_e} \quad (4)$$

where the power output of the cryo-expander (P_e) is subtracted to the compressor power at the denominator. The numerator and the denominator of η_{rt} in Eq. (4) can be written as the product between the air mass flow rate and the specific work of the discharge and charge phases, respectively:

$$P_t - P_{pp} = \dot{m}_{dis} \cdot w_{net,dis} \quad (5)$$

$$P_c - P_e = \dot{m}_{ch} \cdot w_{net,ch} \quad (6)$$

where \dot{m}_{dis} is the air mass flow rate in the discharge phase, \dot{m}_{ch} the air mass flow rate in the charge phase, $w_{net,dis}$ the specific work of the discharge phase and $w_{net,ch}$ the specific work of the charge phase.

The liquid fraction y is defined as the ratio between \dot{m}_{dis} and \dot{m}_{ch} (Eq. (7)):

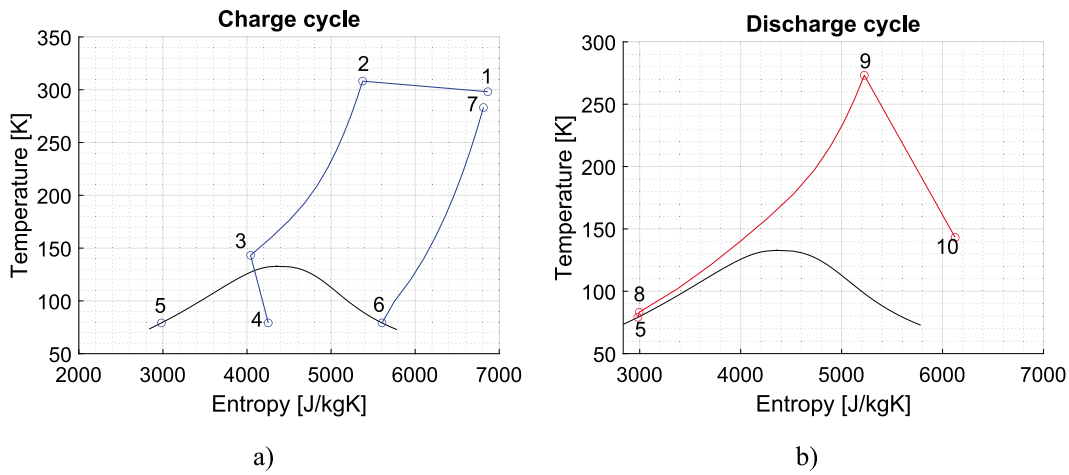


Fig. 3. Temperature–entropy diagrams for charge and discharge phases.

$$y = \frac{\dot{m}_{dis}}{\dot{m}_{ch}} \tag{7}$$

Thus, the round trip efficiency can be further rewritten as:

$$\eta_{rt} = \frac{P_t - P_{pp}}{P_c - P_e} = \frac{w_{net,dis} \cdot y}{w_{net,ch}} \tag{8}$$

According to Eq. (8), the *round trip efficiency* can be maximized by i) decreasing the specific work of the compression during the charge phase; ii) increasing the expansion work during the discharge phase; iii) increasing the liquid fraction y . Starting from the basic system configuration (Fig. 2), more advanced layouts have been proposed in the literature pursuing these three objectives.

3. The LAES configurations in the literature

This Section presents the evolution of the configurations of the LAES system proposed in the literature. It includes the schematics of the layouts, the main available operating parameters and the performance as declared by the authors. For the symbols of the blocks used in the schematics the reader is referred to Table 1A in Appendix A.

Fig. 4 shows the configuration studied by Kishimoto et al. [13], in which a liquefaction plant of the external air supplies directly the liquid air to be stored in the tank. During the discharge phase, the liquid air is first heated up by absorbing heat from the environment, and by recovering heat from the exhaust stream of the second stage of the turbine. Subsequently, it is expanded in the first stage of the turbine, mixed with a fuel burned in a combustion chamber, and finally expanded in the

second stage of the turbine.

Chino et al. [14] first proposed the configuration shown in Fig. 5, in which the key aspect is the inclusion of a heat transfer between charge and discharge phases, in order to further cool down the compressed air and increase the liquid yield. This concept of thermal integration between charge and discharge phases is at the base of all more recently developed configurations. Ameel et al. [43] studied a configuration similar to that in Fig. 5 with the only difference that the discharge cycle

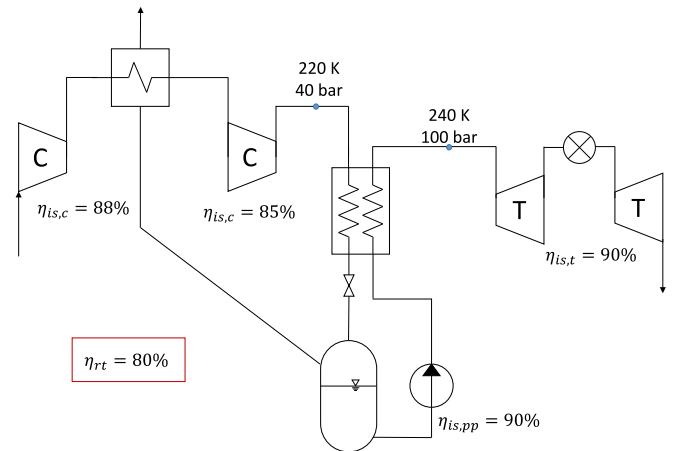


Fig. 5. Configuration proposed by Chino et al. [14].

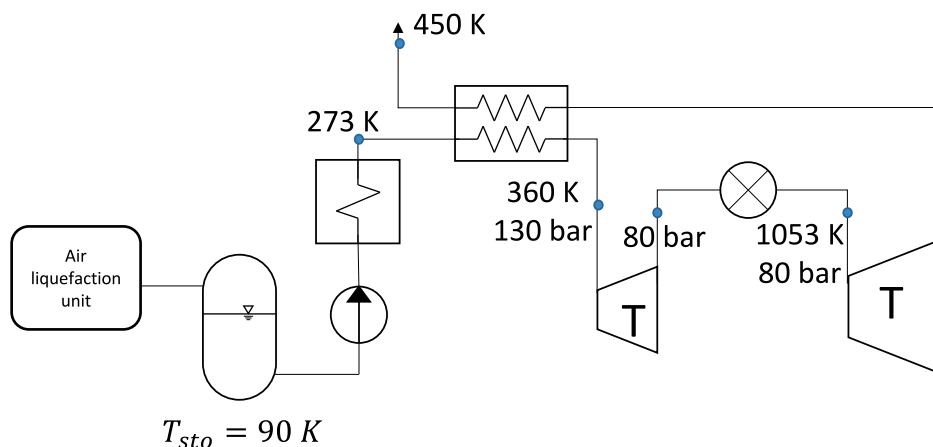


Fig. 4. Configuration proposed by Kishimoto et al. [13].

receives heat entirely from waste heat (available for free at either 300 K or 400 K).

More advanced configurations consider the use of multiple compression and expansion stages, the inclusion of cryogenic expanders in the charge phase (both as a replacement of the throttling valve or as an additional component in a parallel branch of the circuit), and the heat recovery in the discharge phase from heat sources different from environment and fuel combustion. For example, the configuration in Fig. 6 [15] includes all these three ingredients, and is the layout of a pilot plant installed and tested in Slough, United Kingdom. The configuration comprises three compression and four expansion stages, a cryo-expander, in which a fraction of the charge air mass flow rate is expanded, and heaters in the discharge phase that absorb heat from steam supplied from an adjacent power station. It is worth highlighting the thermal integration between the charge and discharge phases, which is given by the heat exchange between liquefying air and exhaust air exiting the last turbine stage.

The common feature of all the configurations presented above (Figs. 4-6) is the exploitation of external heat sources, such as waste heat from industrial processes or heat generated by an adjacent power plant. More recently, research efforts have focused on avoiding the external heat inputs by enhancing the thermal integration between charge and discharge phases, to achieve the so called “stand alone LAES” configuration. An important step forward in this perspective is the configuration in Fig. 7 [17], which includes two separate thermal integrations: the first between the inlet (charge) and the outlet (discharge) of the liquid air tank (blue line loop), the second between compressors coolers (charge) and turbines heaters (discharge) (red line loop). The lack of external heat supply makes the round trip efficiency decrease from values in the range 70 % to 80 % of the previous configurations to 55 %, which, however, is considered by the authors a promising value for the viability of stand-alone LAES systems.

Many other configurations proposed in the literature rely on these two separate thermal integration loops to maximize the heat recovery between charge and discharge phase. They are mainly different from one another for the layout of the liquefaction phase, for the number of compression and expansion stages, and for the exploitation or non-exploitation of the exhaust air coming from the last turbine stage. For example, the configuration suggested by Sciacovelli et al. [19] is very similar to that in [17] except for the more advanced layout of the charge phase. In particular, it comprises three cryo-expanders: the first replaces the throttling valve at the tank inlet, whereas the other two expand a fraction of the recirculated vapour from the tank before it is mixed with the charging air, to further cool it down. The configuration analyzed by Hamdy et al. [20] and shown in Fig. 8 differs for the increased number of

compression and expansion stages, which are equal to 4. Finally, the layout proposed by Tafone et al. [22], shown in Fig. 9, does not recirculate the exhaust air exiting the discharge phase inside the system.

A further evolution step of the LAES system configurations consists in exploiting part of the excess heat deriving from the compression stages in a bottoming power system. The most viable option is that of using an Organic Rankine Cycle (ORC) system. Both References [20, 22] propose the integration of an ORC system within the LAES system to increase the power production. In [20] (Fig. 8), the ORC system is integrated in the following way: the discharge phase of LAES is accomplished using only the first two reheat and turbine stages while the last two become evaporators and turbines of the ORC system. The latter rejects heat to liquid air at the outlet of the liquid air pump so that the cold energy thermal link between charge and discharge phase is no longer necessary. However, the absence of the cold energy recovery between charge and discharge phases leads to a sharp reduction of the LAES performance, which shows a round-trip efficiency of 16.4 %. The ORC system proposed in [22] is placed in the loop of high temperature energy recovery (see the red star in Fig. 9). The ORC system utilizes the excess heat from the compression stages as that in [20] but rejects heat to the environment and not to the cold liquid air. Tafone et al. [22] studied also another possible way to integrate the ORC system, in which the evaporator does not absorb heat downstream of the superheater at the inlet of the first turbine stage (as in Fig. 9) but using a parallel mass flow derivation from the thermal integration between the compressors coolers and turbine heaters. This second layout allows gaining a few percentage points of efficiency in comparison with the first one (53 % vs 50.5 %).

Further modifications of the configurations with an ORC system involve the addition of other thermodynamic systems, such as, for example, a vapour compression cycle (VCC), to exploit the heat rejected by the condenser of the ORC system. This is the case of the configuration proposed by She et al. [21] and shown in Fig. 10, where the ORC system (orange dashed line) is connected in parallel to the high temperature thermal integration loop and the VCC (green dashed-dotted line) is fed by the thermal power released by the ORC condenser. The combination of ORC and VCC resulted in a 5 % improvement of the round trip efficiency (from 50.3 % to 55.5 %) with respect to the baseline LAES (i.e., the configuration without ORC and VCC).

It is clear that the LAES configurations have evolved towards a higher integration between the charging and discharging phases. If we consider the cases where there is no combustion or heat input from outside, i.e., where the heat transfer takes place only with the environment, the roundtrip efficiency is around 10 %. More advanced configurations include a thermal integration (typically with a thermal storage) between the charge and discharge phases reaching roundtrip efficiency of about

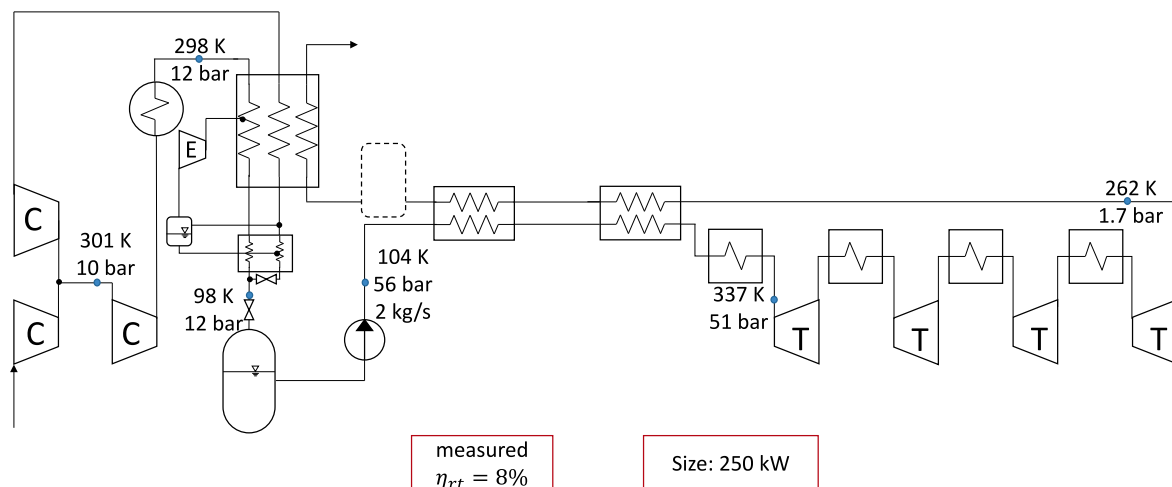


Fig. 6. Configuration proposed by Morgan et al. [15].

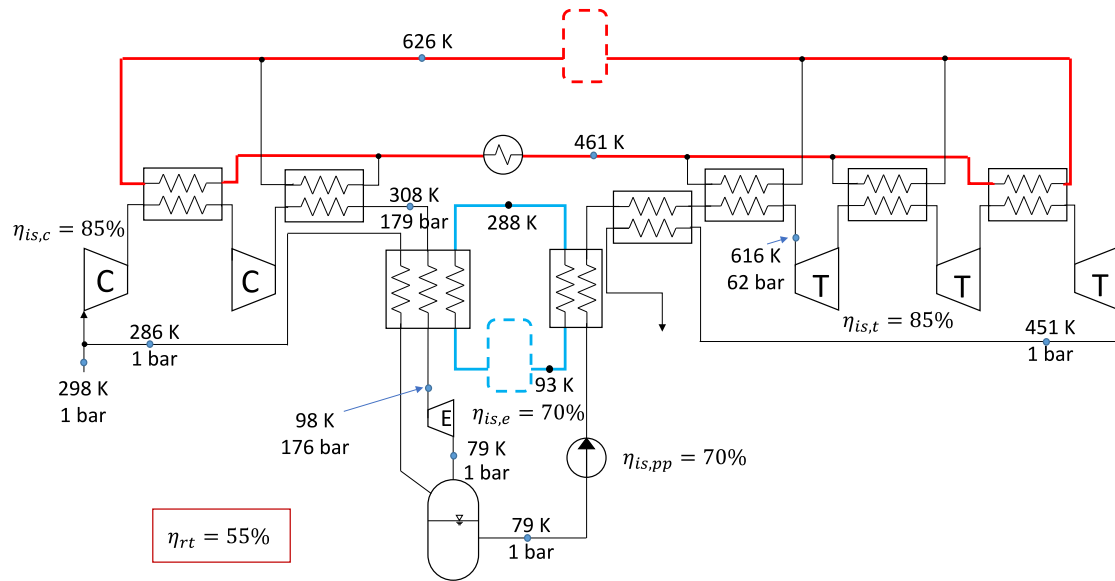


Fig. 7. Configuration proposed by Guizzi et al. [17].

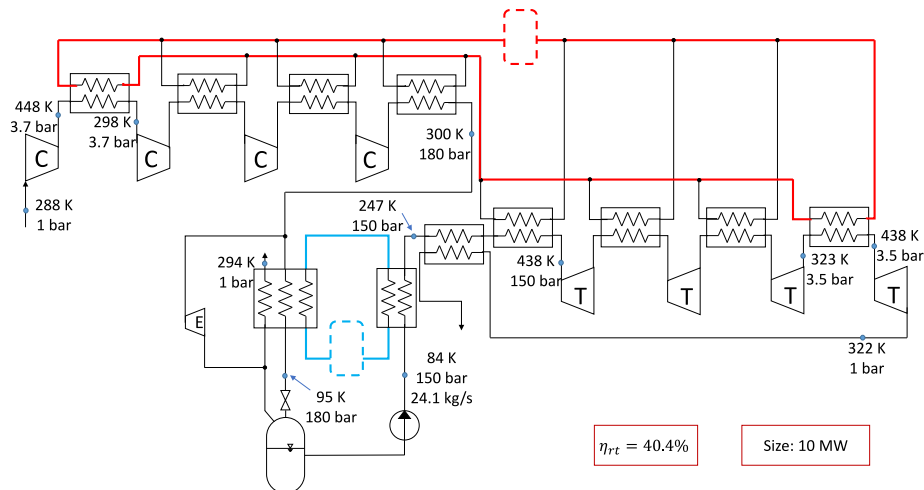


Fig. 8. Configuration proposed in Hamdy et al. [20].

20 % (configuration in Fig. 5 without the external heat inputs) if only one thermal integration circuit is considered, and up to 55 % (configurations in Figs. 7 to 9) in case of multiple integrations. Finally, part of the heat recovered from the compression in the charge phase was used to feed an ORC cycle, which may contribute to a slight increase of the roundtrip efficiency (e.g., from 2 % to 5 % in [22]) depending on the way it is integrated within the system.

4. Identifying a common thread in the evolution of LAES configurations

This Section addresses the evolution of the layouts proposed in the literature, identifying a common thread in their conceptual development. The first step of this evolution is obtained by using different layouts of the liquefaction cycle, while subsequent improvements are based on increasingly higher thermal integration between the charge (liquefaction) and discharge (power generation) phases.

4.1. Absence of thermal integration between charge and discharge phases

The LAES layout described in Section 2 (Fig. 2) shows the simplest

gas liquefaction cycle, i.e., the Linde cycle. Simple modifications of the charging phase layout allow improving the performance of the Linde cycle. These modifications can be simply grouped in two main concepts, which aim to increase the liquid yield at the end of the expansion process (i.e., at the inlet of the tank). Fig. 11 shows these concepts, called Solvay cycle [44] (Fig. 11(a)) and Claude cycle [35] (Fig. 11(b)), respectively. The Solvay cycle (Fig. 11(a)) utilizes a cryo-expander instead of the throttling valve to obtain a higher y . Moreover, the expander contributes to decrease the charging power and in turn to increase the roundtrip efficiency. The Claude cycle adds a splitter in the cooling phase that generates two streams of charging air. The first stream is completely cooled down and then expanded (E1 in Fig. 11(b)), as in the Solvay cycle. The second stream is first partially cooled down, then expanded (E2 in Fig. 11(b)), and finally mixed with the air coming from the storage tank (gas phase) that goes into the heat exchanger to cool down the first stream. This modification helps further cool the air flow entering the tank in order to increase the liquid yield. It is worth pointing out that the Claude cycle is normally presented (see e.g., [11,35]) with a throttling valve in the place of the cryo-expander “E1” in Fig. 11(b). In contrast, in the following, the name “Claude cycle” will exclusively refer to the layout in Fig. 11(b) due to the higher performances of this configuration,

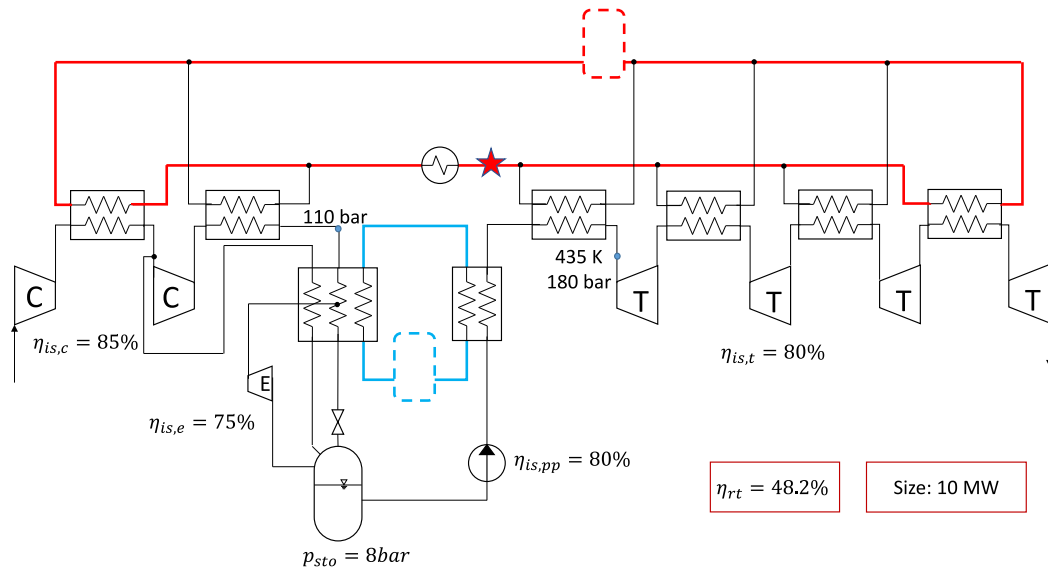


Fig. 9. Configuration proposed by Tafone et al. [22].

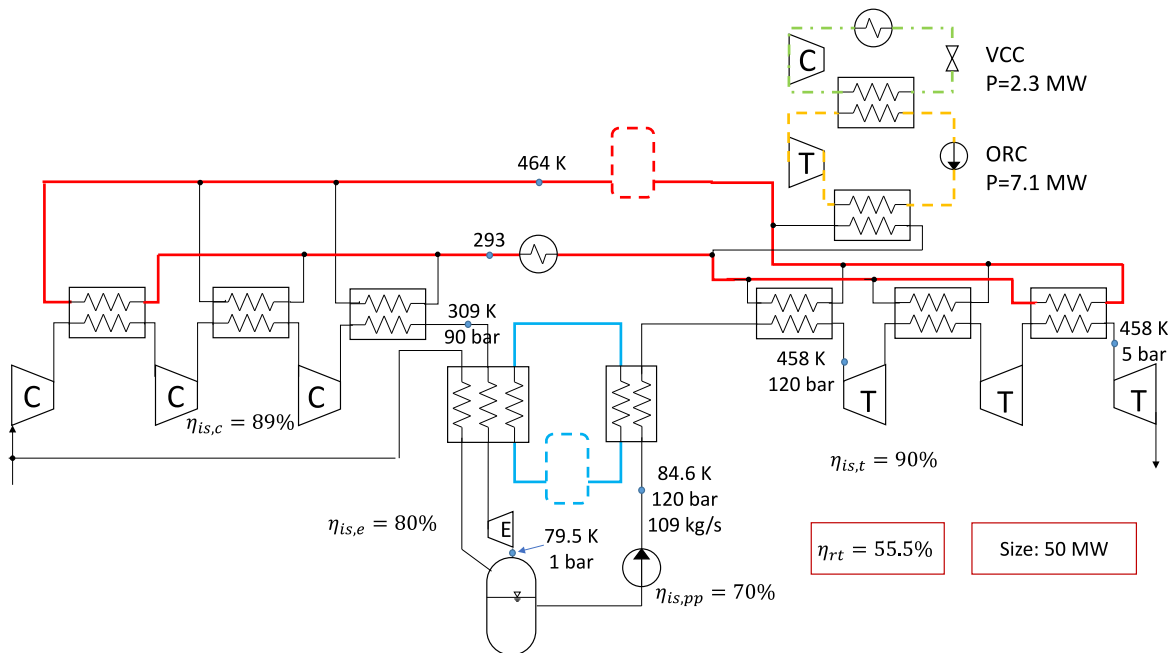


Fig. 10. Configuration proposed by She et al. [21].

as confirmed in [19,45].

To provide a clear picture of the effectiveness of the three types of liquefaction cycles, the performances of the LAES systems of Fig. 2 (Linde cycle), Fig. 11(a) (Solvay cycle) and Fig. 11(b) (Claude cycle) are compared. Table 2 specifies the boundary conditions of this comparison. The models of the components are based on mass and energy balances as specified in Section 5.1. Table 3 reports the liquid yield and the roundtrip efficiency achieved by each liquefaction cycle in the LAES systems mentioned above (i.e., without thermal integration between charge and discharge phases). The Claude cycle shows the highest liquid yield (i.e., 0.270 vs 0.233 of the Solvay cycle and 0.059 of the Linde cycle), which, in turn, results in the highest round trip efficiency (i.e., 10.2 % vs 8.5 % of the Solvay cycle and 1.8 % of the Linde cycle).

4.2. Low temperature thermal integration between charge and discharge phases

The second step to increase the roundtrip efficiency of LAES system relies on a better internal thermal integration between charge and discharge phases. The ambient temperature can be seen as a boundary that divides the system into two possible zones of thermal integration (i.e., above and below such temperature). Considering the Solvay cycle as liquefaction cycle (Fig. 11(a)), Fig. 12 shows that the first simple thermal integration that can be performed by coupling the thermal streams below the ambient temperature. A thermal storage (dashed shape in Fig. 12) can be added to overcome the time mismatch between the charge and discharge phases. The thermal integration below T_{amb} is called in the following “low temperature thermal integration”.

The low temperature thermal integration consists in exploiting not only the heat exchange with the cold vapour (in between points 6 and 7)

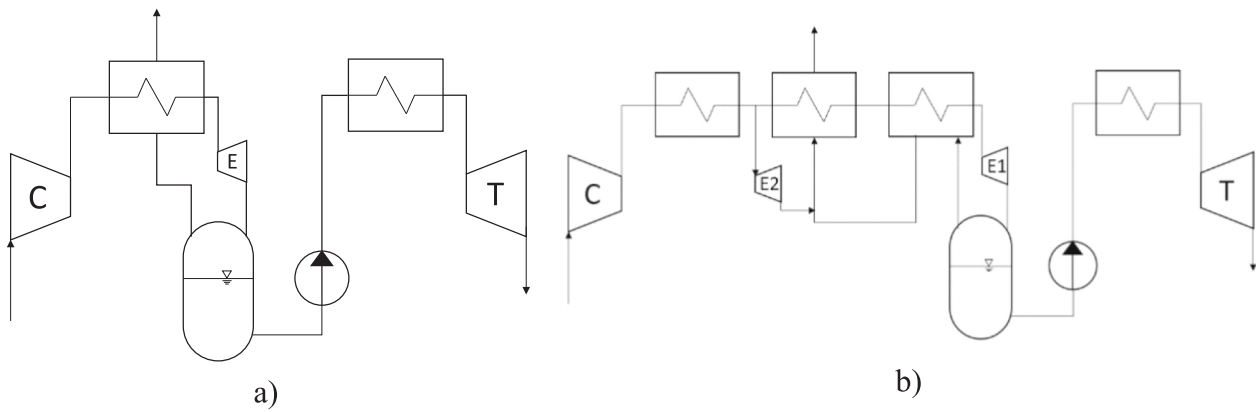


Fig. 11. Layout of LAES with two liquefaction cycles: a) Solvay cycle; b) Claude cycle.

Table 2

Model assumptions for the comparison of the liquefaction cycles in Fig. 11.

T_{amb} [K]	p_{ch} [bar]	p_{dis} [bar]	ΔT_{min} [K]	η_c [-]	η_t [-]	η_e [-]	η_{pp} [-]
298	200	200	10	0.85	0.85	0.70	0.70

Table 3

Liquid yield and roundtrip efficiencies of the different liquefaction cycles (for a LAES system without integration between charge and discharge phases).

Liquefaction cycle	Liquid yield y	Efficiency η_{rt}
Linde	0.059	1.8 %
Solvay	0.233	8.5 %
Claude	0.270	10.2 %

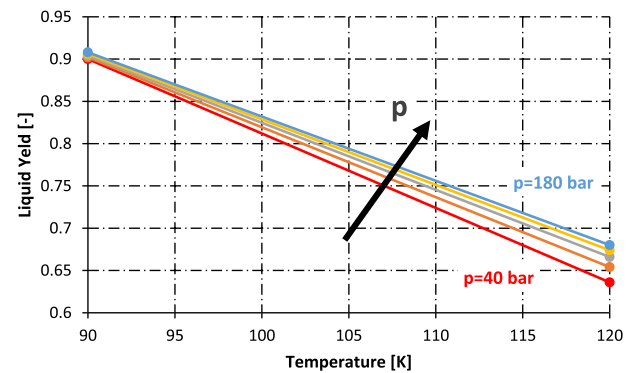


Fig. 13. Liquid yield generated by an adiabatic cryo-expander as a function of the inlet temperature and pressure of air.

function of the cryo-expander inlet temperature and pressure. The cryo-expander inlet temperature heavily influences the liquid yield, which means that reducing this temperature is of utmost importance to have beneficial effects. It is worth observing that, in a thermally integrated LAES, the sum of the thermal capacities of the liquid and vapour fractions (y and $(1 - y)$, respectively) exiting the separation tank is equal to the thermal capacity of the hot compressed air. However, the higher the thermal capacity of the liquid fraction (compared to that of the vapour fraction) the higher the contribution of the heat exchange to the cooling of the compressed air. This is shown in Fig. 14, which compares two T-Q diagrams: the one in Fig. 14(a) refers to the case of heat exchange in absence of thermal integration, i.e., only between the hot compressed air and the vapour returning from the phase separator (between streams 2–3 and 6–7 in Fig. 12), whereas the one in Fig. 14(b) shows the heat transfers in the “three streams heat exchanger” in Fig. 12. The heat transfer between the three streams (one hot and two cold) can be accomplished by splitting the hot stream into two streams, each of which exchanges heat with one of the cold streams. In the case of Fig. 14(a), the higher capacity of the hot stream in comparison with that of the cold vapour stream entails a heat transfer with diverging thermal profiles. On the contrary, the use of two cold streams with different thermal capacities (lower for the cold vapour, points 6–7, and higher for the liquid one, points 5–8) allows to properly match the thermal capacity of the hot stream, resulting in parallel thermal profiles (Fig. 14(b)). This solution

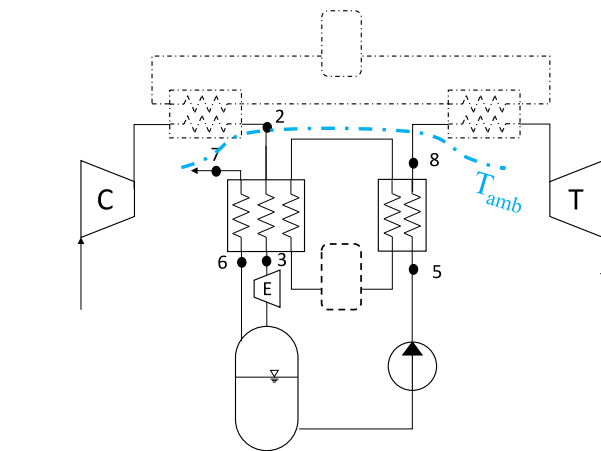


Fig. 12. LAES system layout with a Solvay liquefaction cycle and low temperature thermal integration (the boundary between “low temperature” and “high temperature” sections is highlighted in light blue). (For interpretation of the references to colour in this figure legend, the reader is referred to the web version of this article.)

coming from the separation tank (this is already done in any liquefaction cycle), but also with the cold liquid air from the discharge phase (in between points 5 and 8). In this way, it is possible to reduce the cryo-expander inlet temperature and increase, in turn, the liquid fraction y (the process 3–4 in Fig. 3(a) is lowered). This increase is beneficial for the round trip efficiency, as it appears from the definition in Eq. (8). Typically, thermally integrated LAES systems can achieve liquid yield higher than 60 %. Fig. 13 shows the liquid yield y (generated by an adiabatic cryo-expander with an isentropic efficiency of 70 %) as a

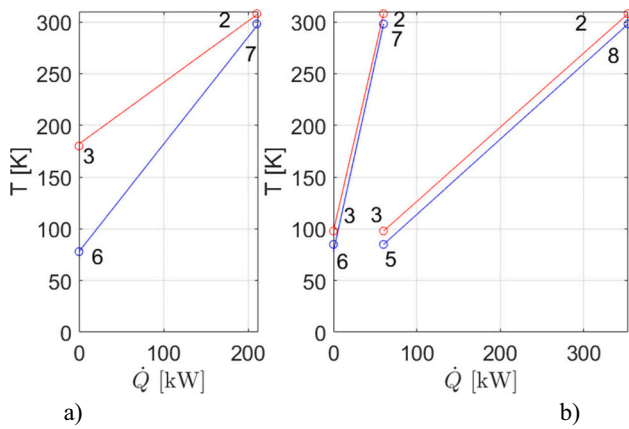


Fig. 14. Temperature–heat transfer rate diagram of the “three streams heat exchanger”. The numbering refers to the layout in Fig. 12.

leads to: i) a higher heat transfer rate, and ii) a strong reduction of the inlet temperature of the cryo-expander (from 180 K to 100 K). Consequently, the liquid yield increases from 0.5 in the case of no thermal integration (Fig. 14(a)) to 0.85 in the case of low temperature thermal integration (Fig. 14(b)).

4.3. Low and high temperature thermal integration between charge and discharge phases

The thermal integration between charge and discharge phases can be extended to the high temperature region (i.e., above the ambient temperature boundary in Fig. 12) to further increase both the liquid yield y and the power output of the turbine in the discharge phase. In fact, air is available at high temperature (after the compression) and high temperature heat is needed to enhance the turbine power output in the discharge phase. Fig. 15 shows the system in Fig. 12 (which included only the low temperature thermal integration) with the addition of the thermal integration section at high temperature. The thermal integration above T_{amb} is called in the following “high temperature thermal integration”. Several works in the literature proved that, in absence of external heat input, the separation between low and high thermal integration is the only way to obtain reasonable roundtrip efficiencies (above 45 %) [17,19,22]. On the contrary, if the only thermal integration below the ambient temperature is used (Section 4.2), the system needs external heat sources to become competitive [14,16].

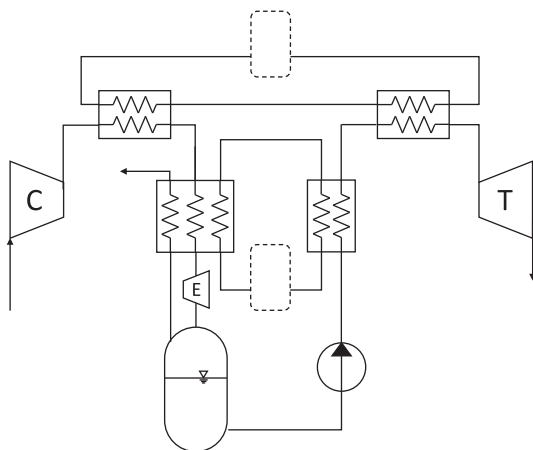


Fig. 15. LAES system layout with a “complete” thermal integration (i.e., low temperature plus high temperature thermal integrations).

4.4. Low and high temperature thermal integration plus a heat recovery system

Further developments of thermal integration consider the inclusion of a heat recovery system exploiting the heat that is still available in the high temperature section, despite the thermal integration. In this context, the most studied heat recovery system is the Organic Rankine Cycle (ORC) system. The ORC system can be thermally coupled to the LAES system by means of the evaporator and the condenser in the two possible ways shown in Fig. 16. In particular, Fig. 16(a) shows that the ORC evaporator absorbs heat from the high temperature integration loop and the condenser rejects heat to the cold liquid fraction in the low temperature section, whereas Fig. 16(b) shows that the ORC evaporator still absorbs heat from the high temperature integration loop, while the condenser rejects heat to the environment. In comparison with the configuration in Fig. 16(b), the one in Fig. 16(a) allows the ORC system to achieve the maximum power production because it exploits the maximum temperature difference between the heat source (above T_{amb}) and the heat sink (below T_{amb}).

However, rejecting heat to the liquid air has the negative effect of reducing the amount of heat that can be exchanged between cold liquid air and hot compressed air in the charge phase. This means that the additional power in the discharge phase coming from the ORC is obtained at the expense of a lower liquid yield in the charge phase. This negative effect is much higher than the gain deriving from the ORC in terms of roundtrip efficiency, as shown by Hamdy et al. [20], where the addition of an ORC system according to the layout in Fig. 16(a) resulted to be detrimental to the roundtrip efficiency of the LAES system. Thus, the most reasonable solution for the integration of the ORC system is the one shown in Fig. 16(b), in which the ORC system receives heat from the high temperature section of the LAES system and the condenser rejects heat to the environment, and not to the LAES discharge phase. The total heat available from the charge cycle (after the compression) always exceeds that absorbed by the air in the discharge cycle. In fact, the mass flow rate through the compressor is higher than that coming from the liquid air tank. Accordingly, the heat recovery by means of ORC systems increases the roundtrip efficiency of LAES. Results of this improvement are shown in [22] where the roundtrip efficiency increased from 48 % to 53 %.

5. Methods

This section introduces to the simulation models (5.1) and addresses the design optimization problem of the LAES systems (5.2).

5.1. Modeling of the LAES system components

The models of the components of the LAES system include mass and energy balances, and equations describing their performance. As regards the turbomachinery, LAES systems include compressors, pumps, turbines and cryo-expanders. The latter are the expanders used in the liquefaction process (Section 4.1). The term “cryo-expander” refers therefore to expanders operating at very low temperature, below the critical point of air. Eqs. (9) and (10) show the mass and energy balances of the turbomachinery components:

$$\dot{m}_{in} = \dot{m}_{out} = \dot{m} \quad (9)$$

$$P_{mec} = \dot{m} \cdot |h_{in} - h_{out}| \quad (10)$$

where \dot{m} [kg/s] is the mass flow rate, h [kJ/kg] is the specific enthalpy and P_{mec} [kW] is the mechanical power output. The performance of turbomachinery is modeled by means of the isentropic efficiencies: Compressors/pumps:

$$\eta_{is} = \frac{(h_{out} - h_{in})_{is}}{h_{out} - h_{in}} \quad (11)$$

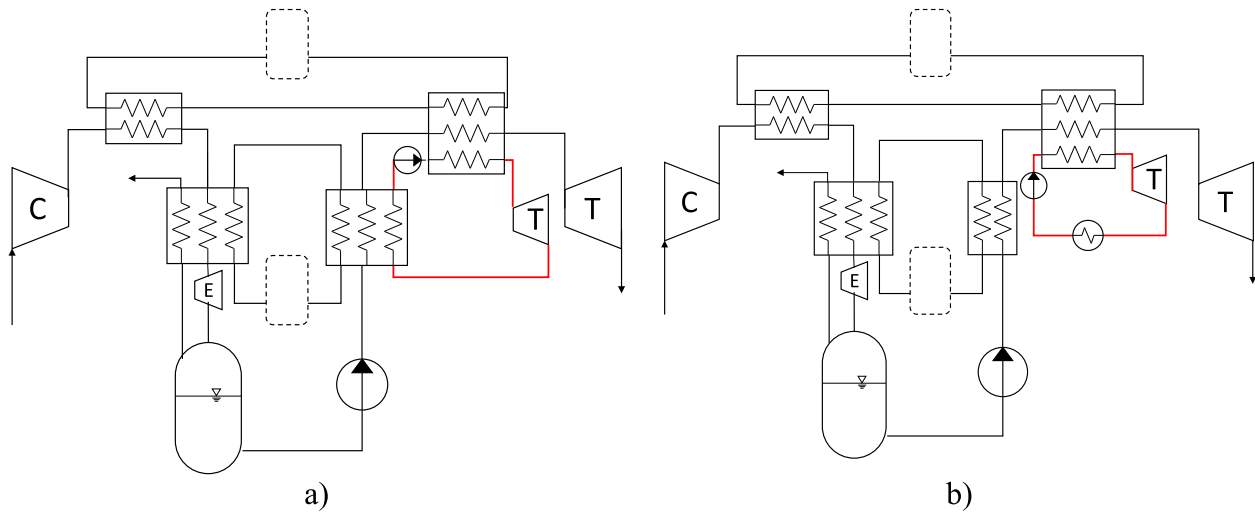


Fig. 16. LAES system layout integrated with an ORC system: a) the evaporator receives heat from the high temperature section of the discharge phase and the condenser rejects heat to the low temperature section of the discharge phase; b) the evaporator receives heat from the high temperature section of the discharge phase and the condenser rejects heat to the environment.

Turbines/cryo-expanders:

$$\eta_{is} = \frac{h_{in} - h_{out}}{(h_{in} - h_{out})_{is}} \quad (12)$$

The mass and energy balances of heat exchangers are provided in Eqs. (13) and (14), respectively,

$$\dot{m}_{1,in} = \dot{m}_{1,out} \text{ and } \dot{m}_{2,in} = \dot{m}_{2,out} \quad (13)$$

$$\dot{m}_{1,in} \cdot (h_{1,in} - h_{1,out}) = \dot{m}_{2,in} \cdot (h_{2,out} - h_{2,in}) = \dot{Q} \quad (14)$$

where \dot{Q} [kW] is the heat transfer rate and the subscripts 1 and 2 refer to the hot and cold fluid, respectively. The heat exchanger performance is considered by defining a minimum temperature difference pinch point (ΔT_{min}) and by imposing a certain pressure drop across it ($\frac{\Delta p}{p}$).

5.2. Design optimization problem

The design optimization problem of a LAES system is:

find \mathbf{x} which maximizes $\eta_{rt}(\mathbf{x})$

$$\text{subject to } \begin{cases} g(\mathbf{x}) = 0 \\ l(\mathbf{x}) > 0 \end{cases} \quad (15)$$

where \mathbf{x} is the array of the decision variables, $\eta_{rt}(\mathbf{x})$ is the objective function to be maximized, and $g(\mathbf{x})$ and $l(\mathbf{x})$ are the equations and inequalities constraints of the design models. The optimization is carried out using a Sequential Quadratic Programming solver provided by the MATLAB Optimization Toolbox [46]. The thermophysical properties of the gas mixture composing air are provided by the REFPROP library [47], which uses the fundamental equations of state developed by Lemmon et al. [48]. The design optimization problem is presented first for application to the configurations proposed in the literature, and then to the “basic configurations” extracted from them, according to the HEATSEP method.

5.2.1. Design optimization of the LAES system configurations proposed in the literature

This Section presents the design optimization of those configurations proposed in the literature (Section 3) that represent better the key steps of thermal integration identified in Section 4.

The case without thermal integration between charge and discharge

phase has already been addressed in Section 4.1 by comparing the three representative liquefaction cycles. Thus, no specific work in the literature is analyzed in this case. The configurations selected for the step of low temperature thermal integration (Section 4.2) are those proposed in [15,16,43]. On the other hand, the step of low and high temperature thermal integration (Section 4.3) is represented better by the configurations in [17,19–22]. Finally, the two configurations in [21,22] are those that lead to a beneficial integration (in terms of round trip efficiency) of an ORC system within the LAES system (Section 4.4).

The design of each selected configuration has been optimized under the same assumptions and boundary conditions. Table 4 reports the performance parameters of the components (Section 5.1) and the environmental conditions. It is worth noting that the isentropic efficiency of the cryo-expander was set conservatively (70 %) because of the relatively low technological maturity of the expanders in the two-phase expansion [49]. As for the configurations including an ORC system, the selected working fluid is R32, which is suitable for the temperature range at which the excess heat is released (20 °C – 150 °C). Moreover, pump and turbine isentropic efficiencies of the ORC systems are equal to those of pump and turbines of the LAES system, respectively (Table 4).

The decision variables of the optimization problem are: the charge (p_{cha}) and discharge (p_{discha}) pressures, the inlet temperature of the expander in the charge phase ($T_{in,exp}$), the inlet temperature of the turbine in the discharge phase ($T_{in,turb}$) and, in the case of Claude cycle (Fig. 11(b)), the ratio between the split and total mass flow rate ($\dot{m}_{split}/\dot{m}_{tot}$), and the temperature of the split mass flow rate (T_{split}). Table 5 shows the lower and upper bounds of the decision variables.

Table 4
Design parameters assumed in the design optimization problem.

Parameter	Value [Unit]
Compressor isentropic efficiency $\eta_{is,c}$	85 [%]
Cryo-expander isentropic efficiency $\eta_{is,e}$	70 [%]
Pump isentropic efficiency $\eta_{is,pp}$	70 [%]
Turbine isentropic efficiency η_{is}	85 [%]
Pinch point ΔT of heat exchangers	10 [K]
Pinch point ΔT of thermal storage heat exchangers	5 [K]
Relative pressure drop of heat exchangers $\Delta p/p$	1 [%]
Ambient temperature T_{amb}	298.15 [K]
Ambient pressure p_{amb}	1 [bar]

Table 5

Decision variables and related lower and upper bounds.

Decision variable	Lower bound	Upper bound	Unit	
1	P_{cha}	40	200	bar
2	P_{dis}	40	200	bar
3	$T_{in,cryo}$	90	150	K
4	$T_{in,nurb}$	400	700	K
5*	$\dot{m}_{split}/\dot{m}_{tot}$	0	0.5	—
6*	T_{split}	200	300	K

* Only for Claude cycle.

5.2.2. Design optimization of the LAES basic configurations according to the HEATSEP method

The application of the HEATSEP method aims at optimizing the exploitation of the internal heat streams within an energy system together with the other design variables. Thus, it appears a very suitable approach for the LAES system, where the internal thermal integration is essential to achieve higher values of roundtrip efficiency (Section 4).

The HEATSEP method [38,39] separates the design optimization problem (Eq. 24) into two subsequent steps:

1. The first step defines the “basic configuration” of the system, which includes only the components different from the heat exchangers and their interconnections [50]. These components are called “basic components”, and, in a LAES system they are: i) compressor; ii) liquid air tank; iii) expander; iv) pump; v) splitter; vi) junction. The thermal links between these “basic components” are then “cut” to make their outlet temperatures independent of the inlet ones in the subsequent components. The temperatures at the extremes of these cuts are added to the set of the decision variables (Table 5) of the design optimization problem of the basic configuration in hand. In this way, the best values of the temperatures of the thermal streams within the system, or, in other words, the best heat transfers between hot and cold internal streams are found. In parallel, the Pinch Analysis [38] is applied to guarantee the feasibility of the heat transfer between internal hot and cold streams, and to have a complete understanding of their optimal interaction. To this end, the optimal heating and cooling requirements of the streams are represented graphically by the cold and hot composite curves, respectively.
2. The second step consists in the design of the Heat Exchangers Network (HEN) (heat exchangers and their interconnections) that performs the optimal internal heat transfers obtained in the first step [51]. The HEN is built following the rules of the Pinch analysis [37] which requires to avoid i) heat transfer across the pinch point; ii) heat rejection to the ambient above the pinch point; iii) external heat input below the pinch point. In the construction of the HEN, the purpose is that of limiting the number of heat exchangers to keep the investment costs low [52].

The completion of the whole procedure (i.e., points 1. and 2. above) for each level of thermal integration identified in Section 4 allows building the configuration that, for that level of thermal integration, exploits at best the internal heat transfers. When the optimal topology and performance of this configuration correspond to those of the associated configuration (i.e., having the same basic components) proposed in the literature, the latter is able to achieve the best match between internal hot and cold streams, otherwise there is still margin for improvement.

6. The basic configurations of LAES according to the HEATSEP method

This Section takes up the LAES system configurations of each thermal integration level identified in Section 4 and shows how a “basic

configuration”, as defined by the HEATSEP method, is “enucleated” from each of them (the results of the optimization of these configurations will be then presented in Section 7). In this procedure the layout of the Claude cycle is the only liquefaction cycle considered in the charge phase because of the highest performance, as discussed in Section 4.1 (Table 3). Only for simplicity of representation, each basic configuration is shown in this Section with only one compression and one expansion stage. However, the impact of a higher number of stages is taken into account in the solution of the HEATSEP optimization problem in Section 7.1.

6.1. Absence of thermal integration between charge and discharge phases

When the thermal integration between the charge and discharge phases is not allowed, there is no advantage in applying the HEATSEP method. The only degree of freedom in this context would be that of modifying the layout of the liquefaction cycle, which, however, has been already widely studied in the literature [11,53]. In particular, the exclusion of the heat exchangers leads to the basic configurations of the liquefaction cycles evaluated in Section 4.1, among which the Claude cycle is the best performing one.

6.2. Low temperature thermal integration between charge and discharge phases

This step of thermal integration allows the heat transfer between charge and discharge phases. However, the possibility of accomplishing internal heat transfers only in the low temperature section of charge and discharge phases makes it necessary to add the constraint that the temperatures associated with the thermal cuts must not exceed the ambient temperature value. Fig. 17 shows the basic configuration of this thermal integration step highlighting the ambient temperature constraint. Heat transfers above the ambient temperature may still occur but only with an external heat source or heat sink (labels “external heat exchange” in Fig. 17). In this work, the external source or sink is the environment. The configurations studied in [14,16,43,54] can be built upon this basic configuration.

6.3. Low and high temperature thermal integration between charge and discharge phases

The basic configuration of this evolutionary step is able to allow the complete thermal integration within the LAES system. Fig. 18 shows this basic configuration highlighting the thermal cuts between the basic components. Compared to the case of low temperature thermal integration (Section 6.2), the basic configuration in Fig. 18 has the same thermal cuts but the HEATSEP optimization approach (Section 5.2.2) is not constrained to consider internal heat transfers only at temperatures

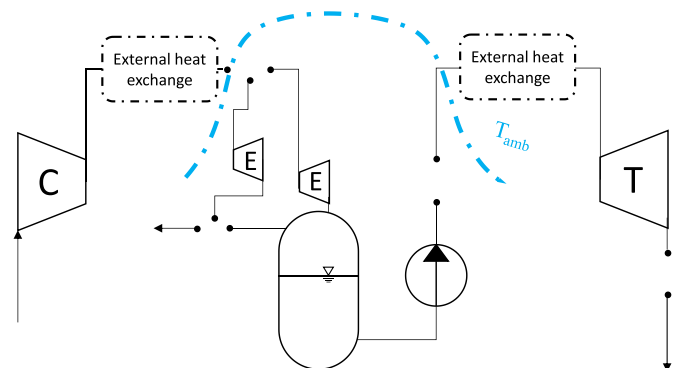


Fig. 17. HEATSEP basic configuration for the low temperature thermal integration step.

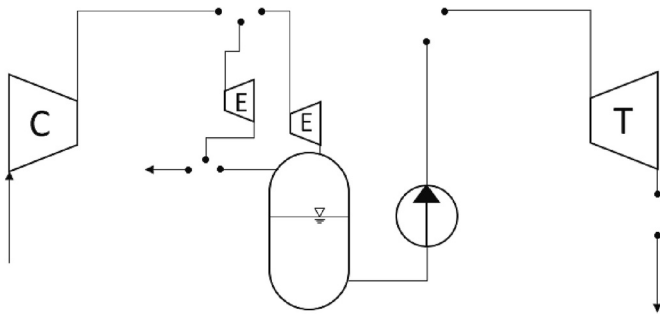


Fig. 18. HEATSEP basic configuration for the low and high temperature integration step.

below the ambient one. The configurations studied in [17,19] can be built upon this basic configuration.

6.4. Low and high temperature thermal integration plus a heat recovery system

The inclusion of an ORC system in the thermal integration scenario entails the inclusion of two more thermal cuts, i.e., those in between the pump and the turbine of the ORC system. Fig. 19 shows the basic configurations of the LAES system (which is the same of Fig. 18) and of the ORC system juxtaposed. The configurations proposed in [20–22] can be built upon this basic configuration.

7. Results of the design optimization

This Section presents and discusses the results of the design optimization applying the HEATSEP method.

To search for the best absolute configuration among all possible ones described in Section 3 while limiting the number of configurations being considered, the two following optimization paths are followed to analyse the influence of the number of compression and turbine stages, and that of the thermal integration, respectively:

- 1) **Influence of the number of compression and expansion stages.** The HEATSEP approach is applied to various basic configurations, all characterized by the most complete thermal integration but different number of stages of the compression and expansion processes, to select the best combination of these stages. The addition of energy recovery systems (ORCs) to LAES systems is neglected at this stage.
- 2) **Influence of the thermal integration level.** The HEATSEP approach is applied to various basic configurations, all characterized by the best combination of compression and expansion stages found at step 1) but different levels of thermal integration, as presented in Section 4.

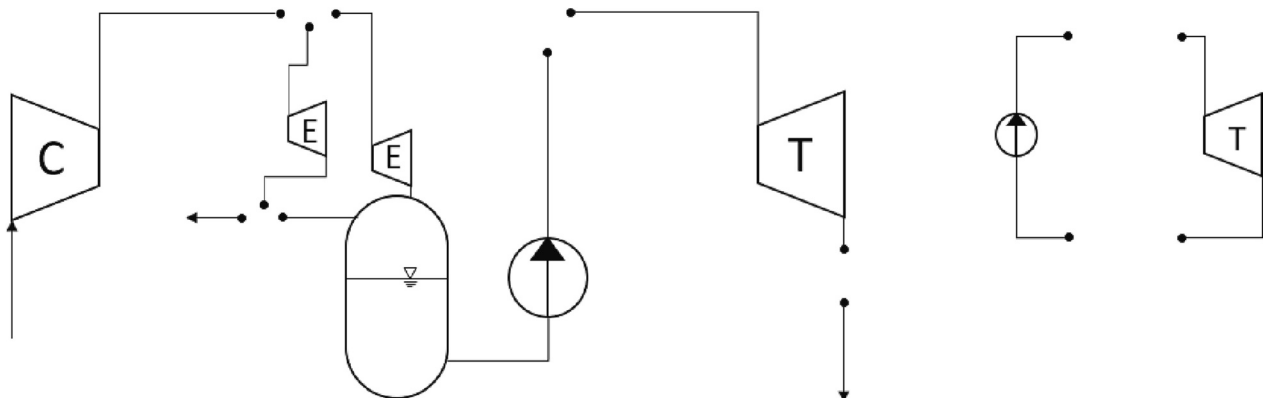


Fig. 19. HEATSEP basic configuration for the step of complete thermal integration in the LAES system plus an ORC system as additional heat recovery system.

The results of the design optimizations carried out at this step are compared to those obtained by optimizing the corresponding configurations proposed in the literature to see whether there could be margin for improvement.

7.1. Influence of the number of compression and expansion stages

The study of the evolution of the literature configurations in Section 4 highlighted that a higher number of compression and/or expansion stages is beneficial for the roundtrip efficiency of the LAES system. The HEATSEP method can be used to quantify how much the roundtrip efficiency can be increased identifying the best combination between the number of compressor and expansion stages. Accordingly, multiple HEATSEP optimizations have been carried out on basic configurations (Section 6) having different combinations of stages. These optimization problems have been solved only for the case of maximum thermal integration within the LAES system (Section 6.3).

Fig. 20 shows the round trip efficiency as a function of the expansion stages for three different numbers of compressors stages. The results point out that the maximum efficiency is achieved when the number of expansion stages is one more than the compression ones. Thus, depending on the number of compression stages, the best combinations compression-expansion stages are: 2–3, 3–4, 4–5 and so on. This finding can be explained by noting that the liquid yield generated during the charging phase is always smaller than 1. Consequently, the air mass flow rate in the discharge phase is lower than that in the charge phase. The inequality of mass flow rates implies that, if the same number of compression and expansion stages is used, the heat generated during the compression processes is always higher than the amount of heat needed to reheat the liquid air before the expansion processes. This situation

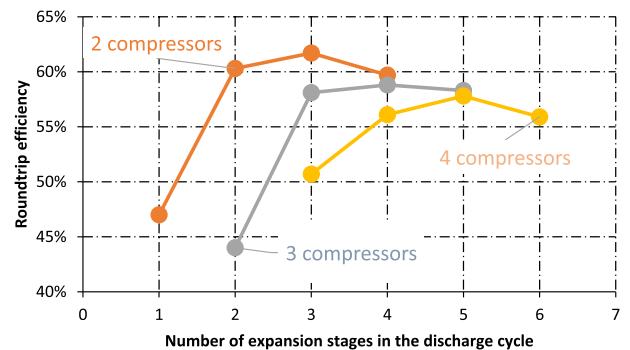


Fig. 20. Results of the HEATSEP optimizations for different combinations of number of compression and expansion stages.

results in a waste of heat and, in turn, to a lower efficiency. For this reason, the use of a higher number of expansion than compression stages generates a higher number of cold streams, which allows higher flexibility and potential to recover the heat excess of the charge phase. This outcome is clarified in Fig. 21, which compares the composite curves obtained with two different combinations of the number of compression and expansion stages, namely, 2–2 (Fig. 21 (a)) and 2–3 (Fig. 21 (b)). The higher number of cold streams in the combination 2–3 entails a better match between hot and cold composite curves and a lower amount of heat rejected to the environment.

Fig. 20 shows also that the maximum values of the roundtrip efficiencies decrease as the staging in the compression phase increases. This is because the higher the compression stages the lower the temperature at which the intercooling heat is provided to the discharge process (i.e., heating before expansion). As a result, the inlet temperatures of the turbines are lower and, in turn, the power output decreases. Thus, the beneficial effect of a better thermal integration obtained with configurations with high number of stages does not compensate for the detrimental effect of the decrease of the turbine inlet temperatures, which heavily influences the roundtrip efficiency [23].

Table 6 reports the values of the turbine inlet temperatures, the outlet temperatures of the last stage of the compressor and the roundtrip efficiencies against the number of compressor and expansion stages. It is apparent that a higher number of compression stages implies a decrease of the temperature at the outlet of the last stage, which, in turn, results in a decrease of the maximum turbine inlet temperatures and of the roundtrip efficiency. It is also important to underline that the staging of turbomachinery is necessary in applications with high pressure ratios (such as LAES systems) because of technological and economic constraints. The selection of the best compromise between round trip efficiency and number of components should therefore consider thermodynamic, economic, and technological aspects.

7.2. Influence of the thermal integration level

The influence of the thermal integration level on the round trip efficiency is analyzed in the following. The last column of Table 7 shows the round trip efficiencies that are obtained by the application of the HEATSEP optimization to the LAES configurations characterized by the optimal combination of two compression stages and three expansion stages found in Section 7.1 and the different level of thermal integration defined in Section 4. The second column of the same Table 7 shows the round trip efficiencies of the literature configurations having the same boundary conditions and the same level of thermal integration. It clearly appears that the efficiency gain obtained using the HEATSEP approach

Table 6

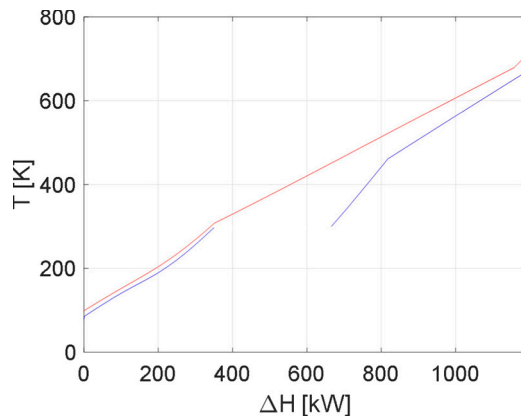
Compressor outlet temperature, turbine inlet temperature and roundtrip efficiency for several combination of compression and expansion stages.

Parameters	Values					
Compression stages	2		3		4	
Compressor T_{out} [K]	704		540		472	
	TIT [K]	η_{rt} [%]	TIT [K]	η_{rt} [%]	TIT [K]	η_{rt} [%]
1 exp. stage	694 K	47.0 %	–	–	–	–
2 exp. stages	694 K	60.3 %	530 K	44.0 %	–	–
3 exp. stages	637 K	61.7 %	516 K	58.1 %	462 K	50.7 %
4 exp. stages	450 K	59.7 %	510 K	58.8 %	462 K	56.1 %
5 exp. stages	–	–	485 K	58.3 %	455 K	57.8 %
6 exp. Stages	–	–	–	–	441 K	55.9 %

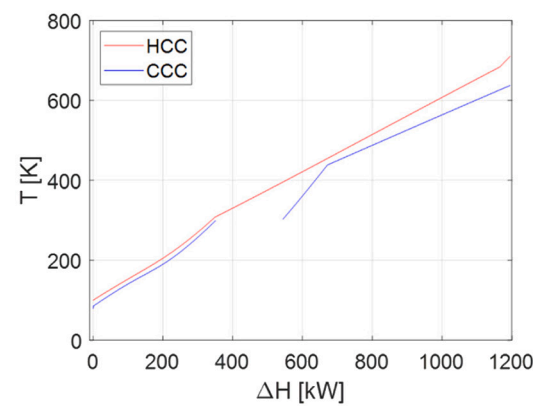
Table 7

Roundtrip efficiency resulting from the design optimization of the literature configurations and of the corresponding basic configurations (HEATSEP method) for different levels of thermal integration between charge and discharge phases.

Evolution steps	Reference	η_{rt} (optimization of the literature layouts)	η_{rt} (Heatsep Optimisation)
Absence of thermal integration	Table	1.8 % 8.5 % 10.2 %	–
Low temperature thermal integration	[43] [16] [15] [17]	19 % 26.3 % 8 % 61.7 %	26.3 %
Low and High temperature thermal integration	[19] [20] [21] [22]	61.1 % 55.0 % 55.3 % 56.3 %	61.7 %
Low and high temperature thermal integration plus ORC system	[21] [22]	61.9 % 59.5 %	64.3 %



a)



b)

Fig. 21. Comparison between composite curves obtained with different combinations of the number of compression and expansion stages: a) 2 compression and 2 expansions stages, b) 2 compression and 3 expansions stages.

becomes significant only for the maximum level of integration. Further improvements can be obtained only by increasing the efficiency of the turbomachinery. It is worth noting that, on the other hand, an increase in the efficiency of heat exchangers only affects the cost of the system. In fact, once the pinch point temperature difference is fixed (Table 4), the optimal heat transfers obtained from optimizing the basic configurations can be carried out by a HEN designed from the resulting composite curves (Section 5.2.2). Each heat exchanger of the HEN can have either a high heat transfer coefficient (and, in turn, low heat transfer area) or a low heat transfer coefficient (and, in turn, high heat transfer area). These alternatives only impact the cost of the heat exchangers and not the round-trip efficiency, which is instead univocally determined once the composite curves are generated.

Looking in more detail:

Absence of thermal integration: in this case the application of the HEATSEP method is omitted, just limiting the analysis to the choice between Solvay and Claude liquefaction systems shown in Section 4.1.

Low temperature thermal integration: The thermal integration in the low temperature section has the great benefit to reduce substantially the liquefaction work. The low roundtrip efficiency found by Morgan et al. [15] is due to the small size of the plant, and to the fact that the cold thermal integration is not completely exploited. Li et al. [16] were able to achieve the lowest liquefaction work ($950 \text{ kJ/kg}_{\text{liquid air}}$). However, the configuration in [16] uses an external high temperature source provided by a nuclear reactor. Fig. 22 shows the basic configuration of the LAES system at this level of thermal integration including the optimal combination of two compression stages and three expansion stages (Section 7.1). It is worth reminding that in this case the HEATSEP optimization approach involves only thermal “cuts” below the ambient temperature (see Section 6.2). Any heat rejection (e.g., heat exchange 2–3) or heat absorption (e.g., heat exchanges 10–11 and 12–13) are towards or from the environment. The optimization of this basic configuration results in the same roundtrip efficiency (26.3 %) of the design optimization of the literature configuration in [16] under the same boundary conditions (i. e., environment as heat source or sink). Fig. 23 shows the composite curves resulting from the HEATSEP method, which coincide with those obtained from the optimization of the configuration in [16]. Below the ambient temperature (i.e., below points 9 and 3), the HEATSEP method achieves an almost perfect thermal integration (i.e., at the minimum ΔT all over the temperature range). However, a big part of heat made available by the hot composite curve (i.e., in between points 2 and 3) is not recovered but rejected to an external heat sink. Starting from the basic configuration in Fig. 22, the construction of the heat exchanger network starting from the composite curves in Fig. 23 leads to the configuration in Fig. 24. The section of low temperature thermal integration is the same as that in [16], demonstrating that the configuration in [16] allows the best internal exploitation of the heat streams available below the ambient temperature (Section 6.2). It is worth observing that, in contrast to the basic configuration in Fig. 22, the configuration in

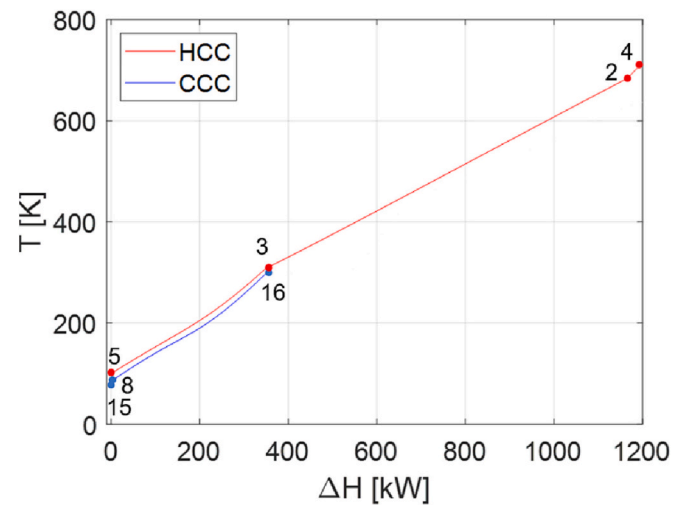


Fig. 23. Composite curves of the “low temperature thermal integration” level resulted from the HEATSEP optimization. These composite curves coincide with those obtained from the optimization of the configuration in [16].

Fig. 24 does not include the cryo-expander in the parallel circuit branch (in between points 4 and 15 in Fig. 22). The exclusion of this expander (derived from the fact that the optimization procedure assigns a zero value to the mass flow rate across the cryo-expander) suggests that the optimal liquefaction cycle in the context of low temperature thermal integration is the Solvay cycle (Fig. 11(a)) and not the Claude cycle (Fig. 11(b)). This result is expected because the higher thermal capacity of the liquid air (Section 4.2) strongly decreases the contribution of the recirculated vapour fraction to the cooling process of the compressed air. This effect cancels the difference between Solvay and Claude cycles in a LAES system in the low temperature thermal integration level.

Low and high temperature thermal integration: The addition of the high temperature thermal storage increases the net power output of the discharge cycle and, in turn, the roundtrip efficiency (maximum η_{rt} of 61.7 % vs 26.3 % of configurations with low temperature integration). Results in Table 7 corresponding to configurations with “low and high temperature thermal integration” highlight a main difference between the η_{rt} of the configurations in [17,19] (above 61 %) and that of the other literature configurations considered in this step (about 55 %). This discrepancy appears because the configurations in [17,19] are the only ones that use the optimal combination of compression and expansion stages identified in Section 7.1 (2 compression and 3 expansion stages).

Fig. 25 shows the basic configuration of the LAES system at this level of thermal integration (Section 6.3), in which every option of thermal integration between the charge and discharge phases is considered by cutting the thermal links between basic components. Fig. 26(a) shows

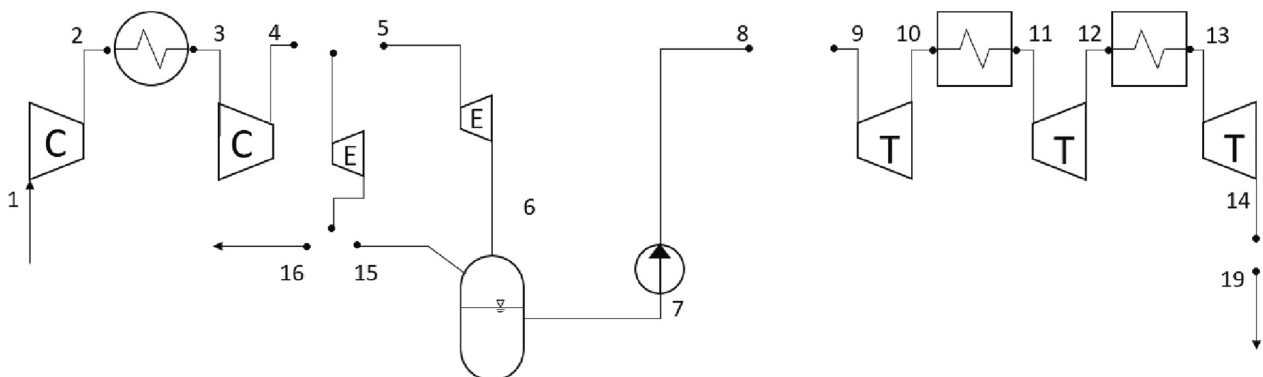


Fig. 22. Basic configuration of the “low temperature thermal integration” level.

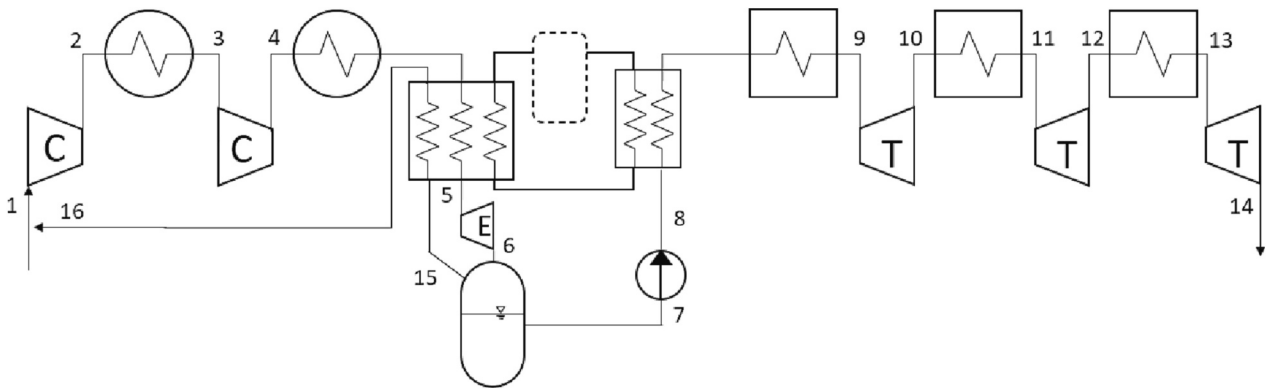


Fig. 24. Layout of the low temperature thermal integrated system built upon the composite curves in Fig. 23.

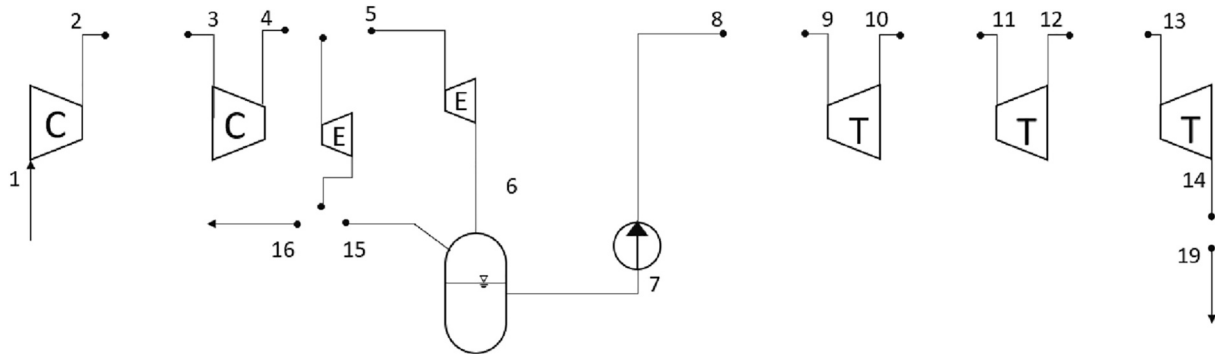


Fig. 25. Basic configuration of the "low and high temperature thermal integration" level.

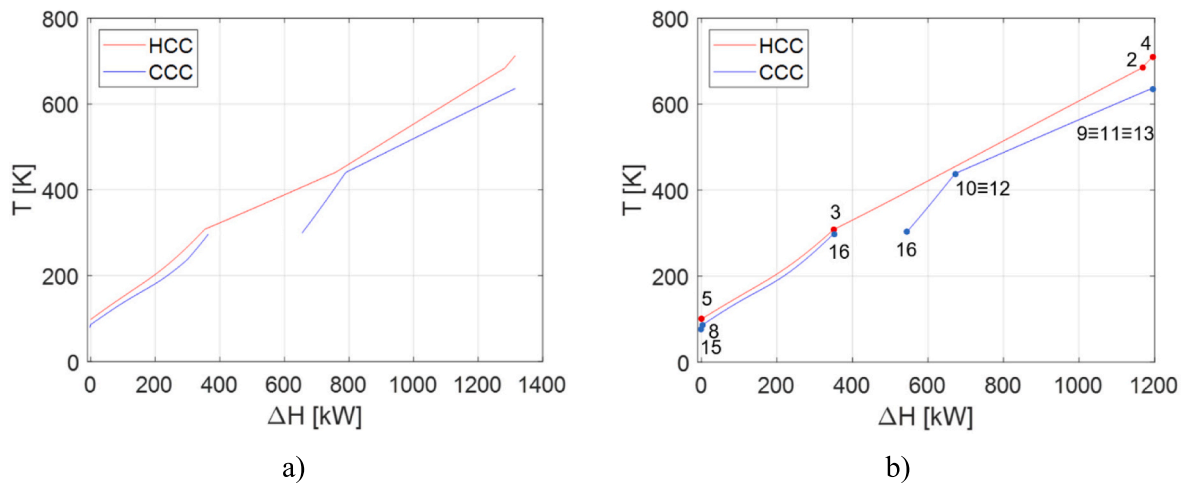


Fig. 26. Comparison between the composite curves of a) the most performing configuration in the literature [17] and b) those resulted from the HEATSEP optimization of the basic configurations in Fig. 25.

the composite curves of the most performing configuration from the literature (i.e., the one in [17]), whereas Fig. 26(b) shows the composite curves resulting from the HEATSEP optimization applied to the basic configuration in Fig. 25. As explained in Section 7.1, the total heat flow in the charge cycle (which is represented by the hot composite curve) is higher than that of the discharge cycle (the cold composite curve). Thus, some amount of heat is inevitably rejected to the environment. Heat rejection in the high temperature section represents a waste of energy, while heat rejection below ambient temperature is not possible. For this reason, the cold composite curve is divided in two parts, with a gap in the middle in correspondence of the ambient temperature, which

represents the heat rejection to the environment. The comparison between the composite curves in Fig. 26(a) and Fig. 26(b) highlights that the application of the HEATSEP method results in a reduction of the amount of heat rejected to the environment. Unlike the configuration in [17], the HEATSEP method suggests avoiding the use of the air flow exiting the last expansion stage to heat up the evaporating air in the discharge phase (Fig. 6). In fact, the use of this thermal stream increases the amount of excess heat available to the discharge phase (in addition to that coming from the charge phase) that must be rejected. The outcome is that of enlarging the gap in the middle of the cold composite curve without affecting the value of η_{rr} , which is 61.7 % for both the

configuration in [17] and the one optimized with the HEATSEP method. Fig. 26 shows the layout obtained by building the heat exchanger network based on the optimal composite curves shown in Fig. 26(b). Compared to that in [17] (Fig. 7), the configuration in Fig. 27 allows removing the heat exchanger that recovers heat from the exhaust air.

Low and high temperature thermal integration plus ORC system: the addition of the ORC system as heat recovery system may help further reduce the amount of heat rejected to the environment (i.e., the gap of the cold composite curve in Fig. 26), which is used to generate additional work. Looking at the results of the literature configurations (Table 7), this solution is slightly beneficial for the roundtrip efficiency, which increases from 0.2 % to 6 % with respect to the configurations without the ORC system. Fig. 28 shows the basic configuration of the LAES system at this evolution step, which is the same as that in Fig. 19 (Section 6.4) except for the addition of the optimal combination of compression and expansion stages. Fig. 29 compares the composite curves of the best performing layout from the literature [21] (Fig. 29(a)) with the composite curves resulting from the HEATSEP method (Fig. 29(b)). The only difference between them is due to the different combination of the number of compression and expansion stages, which, in [21] are 3 and 3 (Fig. 29(a)), whereas in Fig. 29(b) are 2 and 3, respectively. This difference is also the reason why the round trip efficiency obtained with the HEATSEP method is higher (64.3 %) than that of the configuration in [21]. The configuration resulting from the construction of the HEN upon the composite curves of Fig. 29(b) is the same as the one in [21] (Fig. 10) except for i) the vapour compression cycle, which is not considered in this work, and ii) the higher number of compression stages (3 instead of 2).

8. Conclusions

This paper presents a novel approach to analyse Liquid Air Energy Storage systems (LAES) configurations in the literature, which is able to identify a common thread in their evolution and possible design improvements.

Starting from LAES systems where charge and discharge phase are considered separately, the deep analysis of the configurations proposed in the literature allowed different levels of thermal integration to be identified in the evolution towards higher performance. Following an increasing order, these levels are: i) low temperature thermal integration, where only heat fluxes below ambient temperature are exchanged between charge and discharge phases, ii) low and high temperature thermal integration, where a complete thermal integration between charge and discharge phases is considered, and iii) the integration level

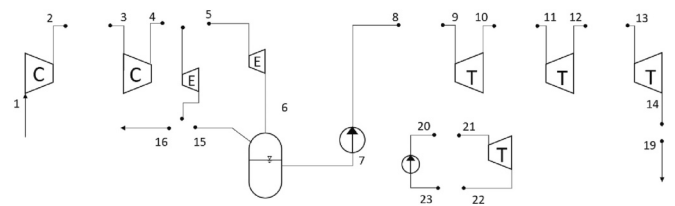


Fig. 28. Basic configuration of the evolution step including “low and high temperature thermal integration” plus the ORC system.

ii) with the addition of an Organic Rankine Cycle system exploiting the excess heat coming from the charge phase. Subsequently, the HEATSEP method is applied, which requires, for each level of thermal integration between charge and discharge phases, the “extraction” of the “basic configuration” (i.e., that including the components different from the heat exchangers) to allow for the search of the optimal match between hot and cold internal thermal streams before defining the configuration of the heat exchangers network. The use of the HEATSEP method is twofold: 1) to identify which combination of the basic components are to be preferred for a given level of thermal integration between charge and discharge phases, and 2) to search for the optimal match between hot and cold internal thermal streams in a given basic configuration corresponding to a specified level of thermal integration between the charge and discharge phases.

The application of the HEATSEP method according to 1) points out that, at the level of complete thermal integration within the LAES system (i.e., low and high temperature thermal integration between the charge and discharge phases), the optimal combination of the number of compression and expansion stages is two compression and three expansion stages. This combination entails an improvement of the round trip efficiency from 1 % to 10 % with respect to other combinations.

On the other hand, for each level of thermal integration between the charge and discharge phases analyzed in 2), the comparison of the design optimization results of the “basic configuration” (HEATSEP method) with those of the systems in the literature built on that basic configuration under the same boundary constraints allowed understanding possible performance improvements deriving from the optimal match between internal hot and cold streams. The following main design guidelines are obtained:

- Thermal integration between the hot streams of the charge phase and the cold ones of the discharge phase is crucial to increase the round

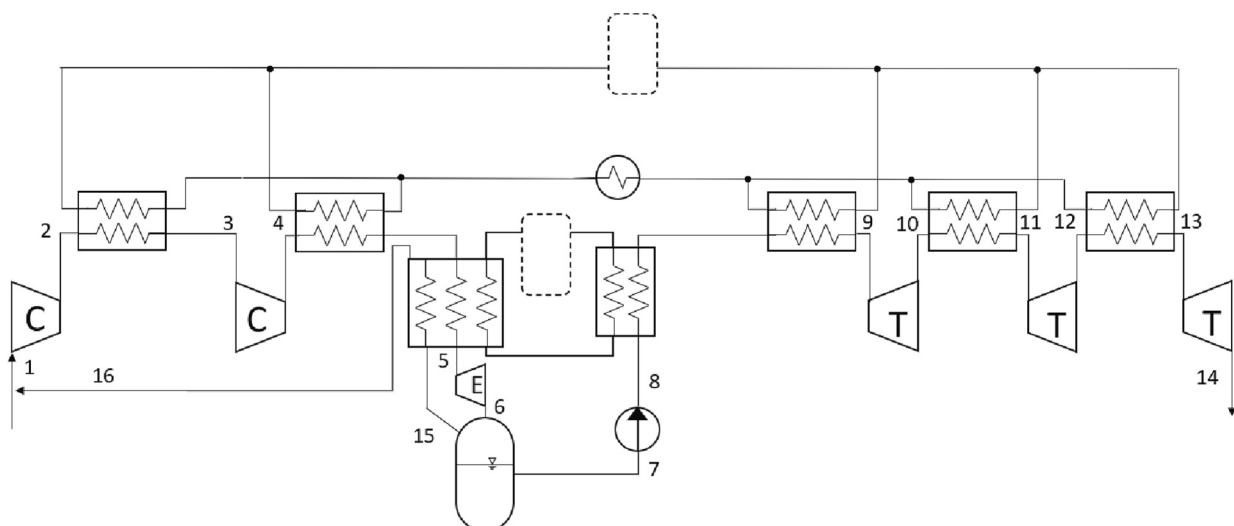


Fig. 27. Layout of the low-and-high temperature thermal integrated system built upon the composite curves in Fig. 26(b).

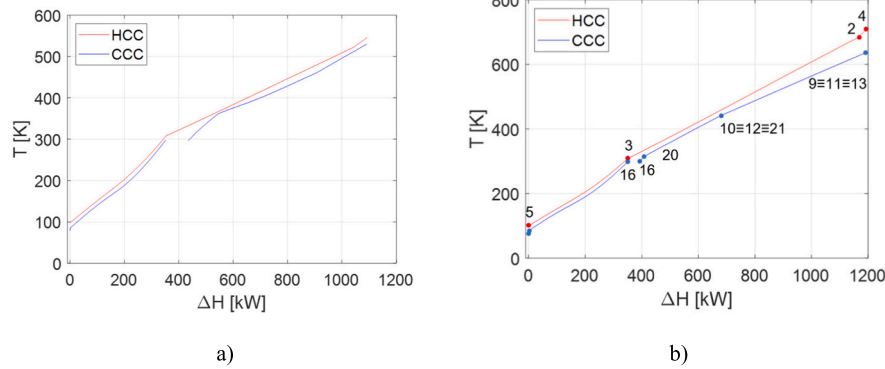


Fig. 29. Comparison between the composite curves of a) the most performing configuration in the literature [21] and b) of those resulted from the HEATSEP optimization of the basic configurations in Fig. 28.

trip efficiency of the LAES system in absence of any external heat input from waste heat sources.

- If the thermal integration between charge and discharge phases is limited to the low temperature section (i.e., below the ambient temperature) and only the environment is used as heat source and sink, a maximum round trip efficiency value of 26.3 % can be achieved.
- The HEATSEP method highlights that the optimal match between internal hot and cold thermal streams in the low temperature thermal integration level makes the Solvay liquefaction cycle performing as the Claude one (in terms of liquid yield) because of the higher contribution of the liquid air to the cooling of the compressed air compared to the recirculated vapour fraction.
- In the low and high temperature thermal integration level, the HEATSEP method suggests avoiding the use of the air flow exiting the last expansion stage to heat up the evaporating air in the discharge phase. This allows building a LAES system configuration that has one less heat exchanger than the best performing literature configuration while maintaining the same round trip efficiency of 61.7 %.
- Compared to a LAES system that exploits at best all internal heat transfers, the inclusion of an Organic Rankine Cycle system as additional heat recovery system leads to an efficiency increase from 61.7 % to 64.3 %.

Although best absolute values of round trip efficiency obtained from the HEATSEP method are higher than those in the literature only for the complete thermal integration level with the Organic Rankine Cycle

system, this work provides the designer with a clear picture of the directions to be taken to achieve higher performance depending on the complexity of the LAES system configuration.

CRedit authorship contribution statement

Gianluca Carraro: Conceptualization, Methodology, Formal analysis, Writing – original draft, Writing – review & editing. **Piero Danieli:** Conceptualization, Visualization, Formal analysis, Writing - original draft, Writing - review & editing. **Tazio Boatto:** Software, Data curation, Writing – original draft. **Andrea Lazzaretto:** Supervision, Methodology, Writing – original draft, Writing – review & editing.

Declaration of competing interest

The authors declare that they have no known competing financial interests or personal relationships that could have appeared to influence the work reported in this paper.

Data availability

Data will be made available on request.

Acknowledgements

This research did not receive any specific grant from funding agencies in the public, commercial, or not-for-profit sectors.









Appendix A

Table 1A
Symbols used in the schematic of the LAES configurations.

Component	Symbol
Compressor	
Turbine	

(continued on next page)

Table 1A (continued)

Component	Symbol
Throttling valve	
Cryo-expander	
Pump	
Heat exchanger	
Cooler (rejects heat to the environment)	
Heater (absorbs heat from the environment)	
Storage tank	
Combustion chamber	

References

- [1] H. Chen, T.N. Cong, W. Yang, C. Tan, Y. Li, Y. Ding, Progress in electrical energy storage system: a critical review, *Prog. Nat. Sci.* 19 (2009) 291–312, <https://doi.org/10.1016/J.PNSC.2008.07.014>.
- [2] IRENA, Electricity storage and renewables: Costs and markets to 2030 132, International Renewable Energy Agency, 2017, ISBN 978-92-9260-038-9.
- [3] A.A. Akhil, G. Huff, A.B. Currier, B.C. Kaun, D.M. Rastler, S.B. Chen, W. D. Gauntlett, DOE/EPRI Electricity Storage Handbook in Collaboration with NRECA (Technical report No: SAND2016-9180647464), 2016, <https://doi.org/10.2172/1431469>. Albuquerque, NM (United States).
- [4] L. Gan, P. Jiang, B. Lev, X. Zhou, Balancing of supply and demand of renewable energy power system: a review and bibliometric analysis, *Sustainable Futures* 2 (2020), 100013, <https://doi.org/10.1016/J.SFTR.2020.100013>.
- [5] G. Volpato, G. Carraro, M. Cont, P. Danieli, S. Rech, A. Lazzaretto, General guidelines for the optimal economic aggregation of prosumers in energy communities, *Energy* 258 (2022), 124800, <https://doi.org/10.1016/J.ENERGY.2022.124800>.
- [6] P. Danieli, A. Lazzaretto, J. Al-Zaili, A. Sayma, M. Masi, G. Carraro, The potential of the natural gas grid to accommodate hydrogen as an energy vector in transition towards a fully renewable energy system, *Appl. Energy* 313 (2022), 118843, <https://doi.org/10.1016/J.APENERGY.2022.118843>.
- [7] S. Rech, A. Lazzaretto, Smart rules and thermal, electric and hydro storages for the optimum operation of a renewable energy system, *Energy* 147 (2018) 742–756, <https://doi.org/10.1016/J.ENERGY.2018.01.079>.
- [8] E. Barbour, I.A.G. Wilson, J. Radcliffe, Y. Ding, Y. Li, A review of pumped hydro energy storage development in significant international electricity markets, *Renew. Sust. Energy. Rev.* (2016) 61, <https://doi.org/10.1016/j.rser.2016.04.019>.
- [9] A.M. Elshurafa, The value of storage in electricity generation: a qualitative and quantitative review, *J Energy Storage* (2020) 32, <https://doi.org/10.1016/j.est.2020.101872>.
- [10] A.V. Olympios, McTigue JD, P. Farres-Antunez, A. Tafone, A. Romagnoli, Y. Li, et al., Progress and prospects of thermo-mechanical energy storage—a critical review, *Progress in Energy* (2020) 3, <https://doi.org/10.1088/2516-1083/abdbba>.
- [11] O. O'Callaghan, P. Donnellan, Liquid air energy storage systems: a review, *Renew. Sust. Energy. Rev.* (2021) 146, <https://doi.org/10.1016/j.rser.2021.111113>.
- [12] E.M. Smith, Storage of electrical energy using supercritical liquid air, *Inst Mech Eng (Lond) Proc* (1977) 191, https://doi.org/10.1243/pime_proc_1977_191_035_02.
- [13] K. Kishimoto, K. Hasegawa, T. Asano, Development of generator of liquid air storage energy system, *Technical Review - Mitsubishi Heavy Industries* 35 (1998).
- [14] K. Chino, H. Araki, Evaluation of energy storage method using liquid air produced by recovery of cold heat, *Nihon Kikai Gakkai Ronbunshu, B Hen/Transactions of the Japan Society of Mechanical Engineers, Part B* (1998) 64, <https://doi.org/10.1299/kikaib.64.884>.
- [15] R. Morgan, S. Nelmes, E. Gibson, G. Brett, Liquid air energy storage - analysis and first results from a pilot scale demonstration plant, *Appl. Energy* 137 (2015) 845–853, <https://doi.org/10.1016/j.apenergy.2014.07.109>.
- [16] Y. Li, H. Cao, S. Wang, Y. Jin, D. Li, X. Wang, et al., Load shifting of nuclear power plants using cryogenic energy storage technology, *Appl. Energy* 113 (2014) 1710–1716, <https://doi.org/10.1016/j.apenergy.2013.08.077>.
- [17] G.L. Guizzi, M. Manno, L.M. Tolomei, R.M. Vitali, Thermodynamic analysis of a liquid air energy storage system, *Energy* 93 (2015) 1639–1647, <https://doi.org/10.1016/j.energy.2015.10.030>.
- [18] H. Guo, Y. Xu, H. Chen, X. Zhou, Thermodynamic characteristics of a novel supercritical compressed air energy storage system, *Energy Convers. Manag.* 115 (2016) 167–177, <https://doi.org/10.1016/j.enconman.2016.01.051>.
- [19] A. Sciacovelli, A. Vecchi, Y. Ding, Liquid air energy storage (LAES) with packed bed cold thermal storage – from component to system level performance through dynamic modelling, *Appl. Energy* 190 (2017) 84–98, <https://doi.org/10.1016/j.apenergy.2016.12.118>.
- [20] S. Hamdy, T. Morosuk, G. Tsatsaronis, Cryogenics-based energy storage: evaluation of cold energy recovery cycles, *Energy* 138 (2017) 1069–1080, <https://doi.org/10.1016/j.energy.2017.07.118>.
- [21] X. She, X. Peng, B. Nie, G. Leng, X. Zhang, L. Weng, et al., Enhancement of round trip efficiency of liquid air energy storage through effective utilization of heat of compression, *Appl. Energy* 206 (2017) 1632–1642, <https://doi.org/10.1016/j.apenergy.2017.09.102>.
- [22] A. Tafone, E. Borri, G. Comodi, M. van den Broek, A. Romagnoli, Liquid air energy storage performance enhancement by means of organic Rankine cycle and absorption chiller, *Appl. Energy* 228 (2018) 1810–1821, <https://doi.org/10.1016/j.apenergy.2018.06.133>.

- [23] A. Tafone, A. Romagnoli, E. Borri, G. Comodi, New parametric performance maps for a novel sizing and selection methodology of a liquid air energy storage system, *Appl. Energy* 250 (2019) 1641–1656, <https://doi.org/10.1016/j.apenergy.2019.04.171>.
- [24] A. Vecchi, Y. Li, P. Mancarella, A. Sciacovelli, Multi-energy liquid air energy storage: a novel solution for flexible operation of districts with thermal networks, *Energy Convers. Manag.* (2021) 238, <https://doi.org/10.1016/j.enconman.2021.114161>.
- [25] X.D. Xue, T. Zhang, X.L. Zhang, L.R. Ma, Y.L. He, M.J. Li, et al., Performance evaluation and exergy analysis of a novel combined cooling, heating and power (CCHP) system based on liquid air energy storage, *Energy* (2021) 222, <https://doi.org/10.1016/j.energy.2021.119975>.
- [26] A. Tafone, Y. Ding, Y. Li, C. Xie, A. Romagnoli, Levelised cost of storage (LCOS) analysis of liquid air energy storage system integrated with organic Rankine cycle, *Energy* (2020) 198, <https://doi.org/10.1016/j.energy.2020.117275>.
- [27] Z. Gao, L. Guo, W. Ji, H. Xu, B. An, J. Wang, Thermodynamic and economic analysis of a trigeneration system based on liquid air energy storage under different operating modes, *Energy Convers. Manag.* (2020) 221, <https://doi.org/10.1016/j.enconman.2020.113184>.
- [28] Q. Liu, Z. He, Y. Liu, Y. He, Thermodynamic and parametric analyses of a thermoelectric generator in a liquid air energy storage system, *Energy Convers. Manag.* (2021) 237, <https://doi.org/10.1016/j.enconman.2021.114117>.
- [29] S. Briola, R. Gabrielli, A. Delgado, Energy and economic performance assessment of the novel integration of an advanced configuration of liquid air energy storage plant with an existing large-scale natural gas combined cycle, *Energy Convers. Manag.* (2020) 205, <https://doi.org/10.1016/j.enconman.2019.112434>.
- [30] S.M. Babaei, M.H. Nabat, F. Lashgari, M.Z. Pedram, A. Arabkoohsar, Thermodynamic analysis and optimization of an innovative hybrid multi-generating liquid air energy storage system, *J Energy Storage* (2021) 43, <https://doi.org/10.1016/j.est.2021.103262>.
- [31] M. Adedeji, M. Abid, M. Dagbasi, H. Adun, V. Adebayo, Improvement of a liquid air energy storage system: investigation of performance analysis for novel ambient air conditioning, *J Energy Storage* (2022) 50, <https://doi.org/10.1016/j.est.2022.104294>.
- [32] C. Wang, Q. Cui, Z. Dai, X. Zhang, L. Xue, Z. You, et al., Performance analysis of liquid air energy storage with enhanced cold storage density for combined heating and power generation, *J Energy Storage* (2022) 46, <https://doi.org/10.1016/j.est.2021.103836>.
- [33] M. Yang, L. Duan, Y. Tong, Y. Jiang, Study on design optimization of new liquified air energy storage (LAES) system coupled with solar energy, *J Energy Storage* (2022) 51, <https://doi.org/10.1016/j.est.2022.104365>.
- [34] M.H. Nabat, S. Sharifi, A.R. Razmi, Thermodynamic and economic analyses of a novel liquid air energy storage (LAES) coupled with thermoelectric generator and Kalina cycle, *J Energy Storage* (2022) 45, <https://doi.org/10.1016/j.est.2021.103711>.
- [35] E. Borri, A. Tafone, A. Romagnoli, G. Comodi, A review on liquid air energy storage: history, state of the art and recent developments, *Renew. Sust. Energ. Rev.* (2021) 137, <https://doi.org/10.1016/j.rser.2020.110572>.
- [36] A. Vecchi, Y. Li, Y. Ding, P. Mancarella, A. Sciacovelli, Liquid air energy storage (LAES): a review on technology state-of-the-art, integration pathways and future perspectives, *Advances, Appl. Energy* (2021) 3, <https://doi.org/10.1016/j.adapen.2021.100047>.
- [37] I. Kemp, Pinch analysis and process integration, *Pinch Analysis and Process Integration* (2006), <https://doi.org/10.1016/B978-0-7506-8260-2.X5001-9>.
- [38] A. Lazzaretto, A. Toffolo, A method to separate the problem of heat transfer interactions in the synthesis of thermal systems, *Energy* 33 (2008) 163–170, <https://doi.org/10.1016/J.ENERGY.2007.07.015>.
- [39] A. Toffolo, A. Lazzaretto, M. Morandin, The HEATSEP method for the synthesis of thermal systems: An application to the S-Graz cycle, *Energy* 35 (2010) 976–981, <https://doi.org/10.1016/J.ENERGY.2009.06.030>.
- [40] G. Carraro, P. Danieli, A. Lazzaretto, T. Boatto, A common thread in the evolution of the configurations of supercritical CO₂ power systems for waste heat recovery, *Energy Convers. Manag.* 237 (2021), 114031, <https://doi.org/10.1016/J.ENCONMAN.2021.114031>.
- [41] M. Morandin, A. Toffolo, A. Lazzaretto, Superimposition of elementary thermodynamic cycles and separation of the heat transfer section in energy systems analysis, *J Energy Resour Technol* (2013) 135, <https://doi.org/10.1115/1.4023099>.
- [42] G. Manente, A. Lazzaretto, Improved layouts and performance of single- and double-flash steam geothermal plants generated by the Heatsep method, *Journal of Energy Resources Technology, Transactions of the ASME* (2020) 142, <https://doi.org/10.1115/1.4047754>.
- [43] B. Ameel, C. T'Joen, K. De Kerpel, P. De Jaeger, H. Huisseune, M. Van Belleghem, et al., Thermodynamic analysis of energy storage with a liquid air Rankine cycle, *Appl. Therm. Eng.* 52 (2013) 130–140, <https://doi.org/10.1016/j.applthermaleng.2012.11.037>.
- [44] V. Gadhiraaju, *Cryogenic Mixed Refrigerant Processes* (2008), <https://doi.org/10.1007/978-0-387-78514-1>.
- [45] K.M. Khalil, A. Ahmad, S. Mahmoud, R.K. Al-Dadah, Liquid air/nitrogen energy storage and power generation system for micro-grid applications, *J. Clean. Prod.* 164 (2017) 606–617, <https://doi.org/10.1016/J.JCLEPRO.2017.06.236>.
- [46] Optimization Toolbox Documentation - MathWorks Italia n.d. <https://it.mathworks.com/help/optim/> (accessed March 8, 2023).
- [47] E.W. Lemmon, I.H. Bell, M.L. Huber, M.O. McLinden, *NIST Standard Reference Database 23: Reference Fluid Thermodynamic and Transport Properties-REFPROP*, 2018.
- [48] E.W. Lemmon, R.T. Jacobsen, S.G. Penoncello, D.G. Friend, Thermodynamic properties of air and mixtures of nitrogen, argon, and oxygen from 60 to 2000 K at pressures to 2000 MPa, *J. Phys. Chem. Ref. Data* 29 (2000) 331, <https://doi.org/10.1063/1.1285884>.
- [49] K. Wang, J. Sun, P. Song, Experimental study of cryogenic liquid turbine expander with closed-loop liquefied nitrogen system, *Cryogenics (Guildf)* (2015) 67, <https://doi.org/10.1016/j.cryogenics.2015.01.004>.
- [50] A. Lazzaretto, F. Segato, Thermodynamic Optimization of the HAT Cycle Plant Structure—Part I: optimization of the “Basic Plant Configuration.”, *J. Eng. Gas Turbine Power* 123 (2001) 1–7, <https://doi.org/10.1115/1.1338999>.
- [51] A. Lazzaretto, F. Segato, Thermodynamic optimization of the HAT cycle plant structure—part II: structure of the heat exchanger network, *J. Eng. Gas Turbine Power* 123 (2001) 8–16, <https://doi.org/10.1115/1.1339000>.
- [52] U.V. Shenoy, Heat exchanger network synthesis: process optimization by energy and resource, *Analysis* 642 (1995).
- [53] C. Yilmaz, T.H. Cetin, B. Ozturkmen, M. Kanoglu, Thermodynamic performance analysis of gas liquefaction cycles for cryogenic applications, *Journal of Thermal Engineering* 5 (2018) 62–75, <https://doi.org/10.18186/THERMAL.513038>.
- [54] Antonelli M, Desideri U, Giglioli R, Paganucci F, Pasini G. Liquid air energy storage: a potential low emissions and efficient storage system. *Energy Procedia*, vol. 88, Elsevier Ltd; 2016, p. 693–7. doi:<https://doi.org/10.1016/j.egypro.2016.6.100>.